NASA TECHNICAL NOTE

NASA TN D-6344

NASA TN D-6344

EXPERIMENTAL AND ANALYTICAL INVESTIGATION OF SUBSONIC LONGITUDINAL AND LATERAL AERODYNAMIC CHARACTERISTICS OF SLENDER SHARP-EDGE 74° SWEPT WINGS

by Edwin E. Davenport and Jarrett K. Huffman

Langley Research Center
Hampton, Va. 23365

NATIONAL AERONAUTICS AND SPACE ADMINISTRATION • WASHINGTON, D. C. • JULY 1971

1. Report No. NASA TN D-6344	2. Government Accession No.	3. Recipient's Catalog No.
4. Title and Subtitle EXPERIMENTAL AND ANALYTICAL INVESTIGATION OF SUBSONIC LONGITUDINAL AND LATERAL AERODYNAMIC CHARACTERISTICS OF SLENDER SHARP-EDGE 74° SWEPT WINGS		5. Report Date July 1971
		6. Performing Organization Code
7. Author(s) Edwin E. Davenport and Jarrett K. Huffman		8. Performing Organization Report No. L-7599
9. Performing Organization Name and Address NASA Langley Research Center Hampton, Va. 23365		10. Work Unit No. 126-13-10-01
		11. Contract or Grant No.
12. Sponsoring Agency Name and Address National Aeronautics and Space Administration Washington, D.C. 20546		13. Type of Report and Period Covered Technical Note
		14. Sponsoring Agency Code

15. Supplementary Notes

16. Abstract

Slender sharp-edge wings having leading-edge sweep angles of 74° have been studied at Mach numbers from 0.2 to 0.8. The wings had arrow, delta, and diamond planforms and were tested at angles of attack from -4° to 30° and angles of sideslip from -8° to 8°. The study consisted of wind-tunnel tests in the Langley high-speed 7- by 10-foot tunnel and predictions of the characteristics by the theories of NASA TN D-3767 and TN D-6243.

17. Key Words (Suggested by Author(s)) Separated flow Thin airfoils Arrow wings Vortex lift		18. Distribution Statement Unclassified — Unlimited	
19. Security Classif. (of this report) Unclassified	20. Security Classif. (of this page) Unclassified	21. No. of Pages 47	22. Price* $3.00

*For sale by the National Technical Information Service, Springfield, Virginia 22151

EXPERIMENTAL AND ANALYTICAL INVESTIGATION OF SUBSONIC
LONGITUDINAL AND LATERAL AERODYNAMIC CHARACTERISTICS OF
SLENDER SHARP-EDGE 74° SWEPT WINGS

By Edwin E. Davenport and Jarrett K. Huffman
Langley Research Center

SUMMARY

Slender sharp-edge wings having leading-edge sweep angles of 74° have been studied at Mach numbers from 0.2 to 0.8, angles of attack from about -4° to 30°, and angles of sideslip from -8° to 8°. The wings had arrow, delta, and diamond planforms. The study consisted of wind-tunnel tests in the Langley high-speed 7- by 10-foot tunnel and predictions of the longitudinal and lateral aerodynamic characteristics by the theories of NASA TN D-3767 and TN D-6243.

The results of the study indicated that the longitudinal characteristics as affected by planform and Mach number could be reasonably well predicted by the leading-edge-suction analogy theories with the exception of the pitching-moment characteristics. With regard to the lateral characteristics, the present analytical method, although an improvement over potential-flow theory, still underpredicted the effective-dihedral parameter for all three planforms.

INTRODUCTION

The advent of supersonic aircraft in recent years has focused attention on thin sharp-edge delta wings and has prompted many theoretical and experimental studies of the vortex-lift characteristics associated with these wings. A promising concept for the calculation of the vortex lift of sharp-edge highly swept wings has been developed at the Langley Research Center of the National Aeronautics and Space Administration. This concept, which is based on a leading-edge-suction analogy, has been applied to wings of various planforms in both incompressible flow and supersonic flow. (See refs. 1 to 3.) From comparisons which have been made between theoretical and experimental data, it has been found that the lift and drag due to lift can be predicted accurately up to the point of vortex breakdown for incompressible flow and supersonic flow. Extension of the leading-edge-suction analogy to include the effects of subsonic compressibility has recently been made in reference 4 for arrow, delta, and diamond wings.

The purpose of the present investigation was to provide a correlation between experimental and theoretical data for slender sharp-edge wings of arrow, delta, and diamond planforms and to study the effects of sideslip angle. The experimental data were obtained in the Langley high-speed 7- by 10-foot tunnel over a Mach number range from 0.2 to 0.8.

SYMBOLS

The results are presented with the longitudinal aerodynamic parameters referred to the stability axes and the lateral aerodynamic parameters referred to the body axes. The origin for these axes is the moment reference center which was at the 50-percent root chord of the 90° trailing-edge wing. (See fig. 1.) This origin was held with respect to the wing apex for the 37° recessed trailing-edge and 37° extended trailing-edge wings. Values are given in both SI Units and U.S. Customary Units. The measurements and calculations were made in the U.S. Customary Units. Conversion factors between SI Units and U.S. Customary Units are presented in reference 5. The symbols are defined as follows:

A   aspect ratio

b   wing span

$\overline{c}$ mean aerodynamic chord of wing

c_R root chord

C_D drag coefficient

ΔC_D drag coefficient due to lift

C_L lift coefficient, $\dfrac{\text{Lift}}{qS}$

C_{L_α} lift-curve slope

C_m pitching-moment coefficient, $\dfrac{\text{Pitching moment}}{qS\overline{c}}$

C_{m_α} pitching-moment-curve slope

C_l rolling-moment coefficient, $\dfrac{\text{Rolling moment}}{qSb}$

C_N normal-force coefficient, $\dfrac{\text{Normal force}}{qS}$

C_n yawing-moment coefficient, $\dfrac{\text{Yawing moment}}{qSb}$

C_s suction coefficient, $\dfrac{\text{Suction force}}{qS}$

C_Y side-force coefficient, $\dfrac{\text{Side force}}{qS}$

C_{l_β} effective-dihedral parameter, $\dfrac{\Delta C_l}{\Delta \beta}$

C_{n_β} directional-stability parameter, $\dfrac{\Delta C_n}{\Delta \beta}$

C_{Y_β} side-force parameter, $\dfrac{\Delta C_Y}{\Delta \beta}$

K_p constant in potential-flow-lift term

K_v constant in vortex-lift term

L/D lift-drag ratio

M free-stream Mach number

q free-stream dynamic pressure

R Reynolds number per meter

S reference wing area

α angle of attack, deg

β angle of sideslip, deg

$\dfrac{\Delta y}{b/2}$ center-of-pressure location

Subscripts:

p   potential-flow-lift contribution

v   vortex-lift contribution

t   total contribution

MODEL DESCRIPTION

Photographs of one model (diamond planform) mounted in the tunnel and the trailing-edge components of the other two models (arrow and delta planforms) are shown as figure 2. The physical characteristics and dimensions of the models are presented in figure 1. Pertinent geometric characteristics are given in table I.

The model forward portion comprising the main forward wing and balance housing was machined from solid aluminum. The three interchangeable wing—balance-housing portions were also machined from solid aluminum and were bolted to the forward portion for a complete model. The wings were thin flat-plate airfoils with sharp tapered edges.

TESTS, APPARATUS, AND CORRECTIONS

The investigation was made in the Langley high-speed 7- by 10-foot tunnel which is a rectangular, atmospheric, single-return wind tunnel. Tests were conducted over a Mach number range from 0.2 to 0.8, a nominal angle-of-attack range from about -4° to 30°, and an angle-of-sideslip range from -8° to 8° at $\alpha = 4^O$ and $\alpha = 12^O$. The approximate variation of the test Reynolds number per meter with Mach number is shown in figure 3.

Force and moment measurements were made with a six-component internally mounted strain-gage balance. Angles of attack and sideslip were corrected for sting deflection. Axial force was corrected to a condition of free-stream static pressure acting on the base of the model and the balance cavity. Jet-boundary corrections and blockage corrections, which were applied to the data, were obtained by the methods of references 6 and 7, respectively. No artificial transition was used on the models.

RESULTS AND DISCUSSION

In the discussion of the results of the investigation, the 90° trailing-edge configuration, the 37° recessed trailing-edge configuration, and the 37° extended trailing-edge configuration are referred to as the delta wing, the arrow wing, and the diamond wing, respectively.

4

Longitudinal Aerodynamic Characteristics

The basic longitudinal aerodynamic characteristics for the three wings at zero sideslip are shown in figure 4. These data show no significant differences in the lift and drag characteristics of the three wings although the aspect ratios are not the same. The lift curves show an increase in C_{L_α} for all models for all Mach numbers above an angle of attack of about 5°. This nonlinearity is due to the lift contributed by the leading-edge vortex. The pitching-moment curves show that C_{m_α} becomes less negative as wing area at the trailing edge is removed and more negative as wing area is added. Also, C_{m_α} was seen to become more negative as Mach number increased. All three models exhibited about the same values of L/D for all Mach numbers as can be seen in figure 5.

The longitudinal aerodynamic characteristics obtained at a sideslip angle of 4° show the same general trends observed at zero sideslip. (See figs. 4 and 6.)

Lateral Aerodynamic Characteristics

The variation of the lateral stability derivatives C_{l_β}, C_{n_β}, and C_{Y_β} with angle of attack is shown in figure 7 for a sideslip angle increment of 4°. The effective-dihedral parameter was positive $\left(-C_{l_\beta}\right)$ for all models at all Mach numbers and was essentially linear with increase in α. This parameter was relatively unaffected by Mach number. The effects of trailing-edge modification on the side-force derivative C_{Y_β} were minor except at the lowest test Mach number (M = 0.2). Values of C_{Y_β} generally remained within ±0.002 over most of the angle-of-attack range for all Mach numbers. The lateral aerodynamic coefficients C_l, C_n, and C_Y as a function of sideslip angle were determined for a Mach number of 0.4 and are shown in figure 8 to be essentially linear with sideslip angle for both $\alpha = 4^O$ and 12°.

Comparison of Theoretical and Experimental Data

The method used to obtain theoretical lift and drag-due-to-lift coefficients was developed in references 1 to 4. The expression used to obtain total theoretical lift coefficient $\left(C_L\right)_t$ is

$$\left(C_L\right)_t = K_p \sin \alpha \, \cos^2\alpha + K_v \cos \alpha \, \sin^2\alpha$$

Values of K_p and K_v were obtained by the method of reference 4. Comparison of the experimental data with data obtained by using this theory is made in figures 9(a), (b), (c), and (d) for M = 0.2, 0.4, 0.6, and 0.8, respectively. Both the potential-flow-theory lift coefficient $\left(C_L\right)_p$ and the total lift coefficient $\left(C_L\right)_t$, which includes the theoretical vortex-lift effect, are shown. The theoretical results are in excellent agreement with the experimental results for the delta wing and in reasonably good agreement for the diamond

and arrow wings. Although the effects of Mach number are rather small for these slender wings, the experimental results indicate that the large vortex-lift effect predicted by the theory are maintained up to the highest Mach number of the tests. The reduction of lift for the arrow wing and the increase in lift for the diamond wing at the higher angles of attack relative to the theory is discussed in reference 3.

Comparison of theoretically and experimentally obtained values of drag due to lift $\frac{\Delta C_D}{C_L{}^2}$ as a function of C_L is made in figure 10. For zero leading-edge suction, it can be shown (ref. 3) that $\frac{\Delta C_D}{C_L{}^2} = \frac{\tan \alpha}{(C_L)_t}$. The short-dash curves represent $\frac{\Delta C_D}{(C_L)_p^2}$ which corresponds to the condition of potential lift only $\left(\text{that is, } (C_L)_p = K_p \sin \alpha \cos^2\alpha\right)$, whereas the solid curves represent $\frac{\Delta C_D}{(C_L)_t^2}$ (vortex plus potential). Some of the discrepancy between theoretical and experimental values of lift are reflected in the drag-due-to-lift curves at $M = 0.2$ and 0.4 where theory underpredicts drag for the arrow wing and overpredicts drag for the diamond wing. At $M = 0.6$ and 0.8 the agreement has become better and there is less effect of planform. This same trend was noted for the lift curves (fig. 9). The long-dash lines of constant value represent drag for potential flow with full leading-edge suction $\left(\frac{1}{\pi A}\right)$. The increment between the $\frac{1}{\pi A}$ curves and the curves for drag with total lift $\left((C_L)_p + (C_L)_v\right)$ gives some indication of the drag penalty associated with leading-edge separation. It should be noted, however, that the penalty is substantially less than that indicated by zero suction theory with vortex lift ignored. A similar comparison of these parameters is made in reference 3.

An attempt was made to predict the variation of C_m with α. The results are presented in figure 11. The expression used to obtain the total theoretical pitching-moment coefficient is

$$(C_m)_t = (C_N)_p\left(\frac{\Delta x}{c_R}\right)_p\left(\frac{c_R}{\bar{c}}\right) + (C_N)_v\left(\frac{\Delta x}{c_R}\right)_v\left(\frac{c_R}{\bar{c}}\right)$$

where

$$(C_N)_p = K_p \sin \alpha \cos \alpha$$

$$(C_N)_v = K_v \sin^2\alpha$$

$\left(\frac{\Delta x}{c_R}\right)_p$ nondimensional longitudinal distance between center of potential-flow lift and moment center

$\left(\dfrac{\Delta x}{c_R}\right)_v$ nondimensional longitudinal distance between center of vortex lift and moment center

The values of $\left(\dfrac{\Delta x}{c_R}\right)_p$ and $\left(\dfrac{\Delta x}{c_R}\right)_v$ were estimated by assuming that they were equivalent to the values obtained in potential flow for lift and leading-edge thrust, respectively; the method of reference 8 was used.

Fairly good agreement between theoretical and experimental values of C_m was obtained at $M = 0.6$ and $M = 0.8$ for the delta wing over the complete angle-of-attack range (figs. 11(c) and 11(d)). A possible explanation for the poor agreement for the arrow wing is that there is insufficient area in the tip region on which the suction near the tip can be converted to vortex lift. (See ref. 3.) It is likewise possible that additional vortex lift is produced on the aft extension of the diamond wing. Corresponding agreement for the arrow and diamond wings appears to show about the same trends shown for the variation of C_L with α (fig. 9).

Comparison of predicted and experimental values of effective-dihedral parameter C_{l_β} is made in figure 12. The predicted C_{l_β} was obtained by calculating the rolling-moment coefficient at $\beta = 5^O$ for both the potential flow and the vortex flow and then combining the results; that is,

$$\left(C_l\right)_t = \left(C_l\right)_p + \left(C_l\right)_v$$

where

$$\left(C_l\right)_p = \frac{C_l}{C_L}\left(K_p \sin\alpha \cos^2\alpha\right)$$

$$\left(C_l\right)_v = \frac{1}{2}\left[\left(C_s\right)_{left}\left|\frac{\Delta y}{b/2}\right|_{left} - \left(C_s\right)_{right}\left|\frac{\Delta y}{b/2}\right|_{right}\right]\sin^2\alpha \cos\alpha$$

and C_s is suction coefficient.

Values of $\dfrac{C_l}{C_L}$, C_s, K_p, and $\dfrac{\Delta y}{b/2}$ were obtained from a Wagner program (ref. 8). Although the theory consistently underpredicted the experimental results, the inclusion of the vortex-flow term does provide an improvement over the potential-flow theory. Whether this underprediction of the effective-dihedral parameter is associated primarily with inadequacies in the method of predicting the leading-edge-suction distribution or with the fact that such effects as redistribution of the potential-flow lift or vortex breakdown are not accounted for is not known, and further study is needed.

7

CONCLUSIONS

On the basis of results of an experimental and analytical study of the subsonic aerodynamic characteristics of slender sharp-edge wings having a leading-edge sweep angle of 74°, the following conclusions can be stated:
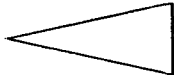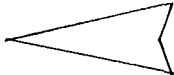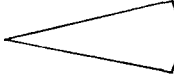
1. The aerodynamic characteristics were only moderately affected by Mach number M over the test range (M = 0.2 to 0.8).

2. With the exception of pitching-moment characteristics, the longitudinal characteristics as affected by planform and Mach number were well predicted by the leading-edge-suction analogy.

3. Leading-edge-suction analogy accurately predicted pitching moments for the delta wing, but there was poor agreement between theoretical and experimental data for the arrow and diamond wings.

4. The application of the leading-edge-suction analogy to predict the effective-dihedral parameter resulted in an improvement over predictions by potential-flow theory. However, the theory still underpredicted the magnitude, and further study is needed.

Langley Research Center,
National Aeronautics and Space Administration,
Hampton, Va., June 15, 1971.

8

REFERENCES

1. Polhamus, Edward C.: A Concept of the Vortex Lift of Sharp-Edge Delta Wings Based on a Leading-Edge-Suction Analogy. NASA TN D-3767, 1966.

2. Polhamus, Edward C.: Application of the Leading-Edge-Suction Analogy of Vortex Lift to the Drag Due to Lift of Sharp-Edge Delta Wings. NASA TN D-4739, 1968.

3. Polhamus, Edward C.: Predictions of Vortex-Lift Characteristics by a Leading-Edge Suction Analogy. J. Aircraft, vol. 8, no. 4, Apr. 1971, pp. 193-199.

4. Polhamus, Edward C.: Charts for Predicting the Subsonic Vortex-Lift Characteristics of Arrow, Delta, and Diamond Wings. NASA TN D-6243, 1971.

5. Mechtly, E. A.: The International System of Units — Physical Constants and Conversion Factors (Revised). NASA SP-7012, 1969.

6. Gillis, Clarence L.; Polhamus, Edward C.; and Gray, Joseph L., Jr.: Charts for Determining Jet-Boundary Corrections for Complete Models in 7- by 10-Foot Closed Rectangular Wind Tunnels. NACA WR L-123, 1945. (Formerly NACA ARR L5G31.)

7. Herriot, John G.: Blockage Corrections for Three-Dimensional-Flow Closed-Throat Wind Tunnels, With Consideration of the Effect of Compressibility. NACA Rep. 995, 1950. (Supersedes NACA RM A7B28.)

8. Wagner, Siegfried: On the Singularity Method of Subsonic Lifting-Surface Theory. AIAA Paper No. 69-37, Jan. 1969.

TABLE I.- GEOMETRIC CHARACTERISTICS

Configuration	Span		$\bar{c}$		Area		Aspect ratio
	centimeters	inches	centimeters	inches	meters^2	feet^2	
90° T.E.	58.27	22.94	67.72	26.66	0.2960	3.186	1.147
37° Recess. T.E.	58.27	22.94	53.11	20.91	0.2320	2.498	1.463
37° Ext. T.E.	58.27	22.94	81.69	32.16	0.3600	3.875	0.943

74°

50 80 (20.00)

101.60 (40.00)

90° Trailing edge

58.27 (22.94)

Center of moments

74°

2 13 (0 84)

37°

50 80 (20.00)

2 84 (1 12)

101 60 (40 00)

37° Recessed trailing edge

5.26 (2.07)

58 27 (22.94)

74°

37°

0 71 (0 28)

50 80 (20.00)

120.02 (47.25)

58.27 (22.94)

37° Extended trailing edge
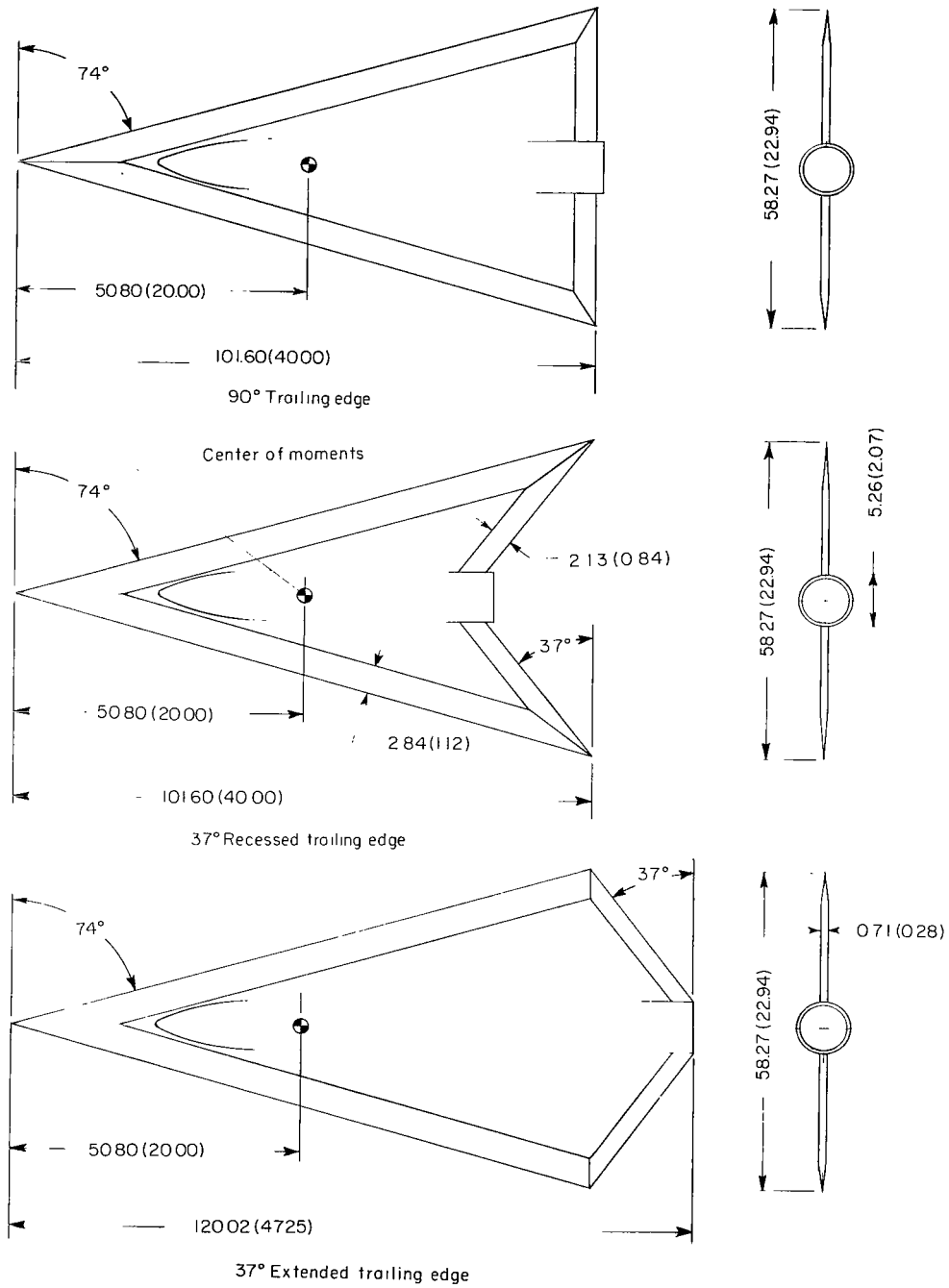
Figure 1.- Details of models. Linear dimensions are in centimeters (inches).
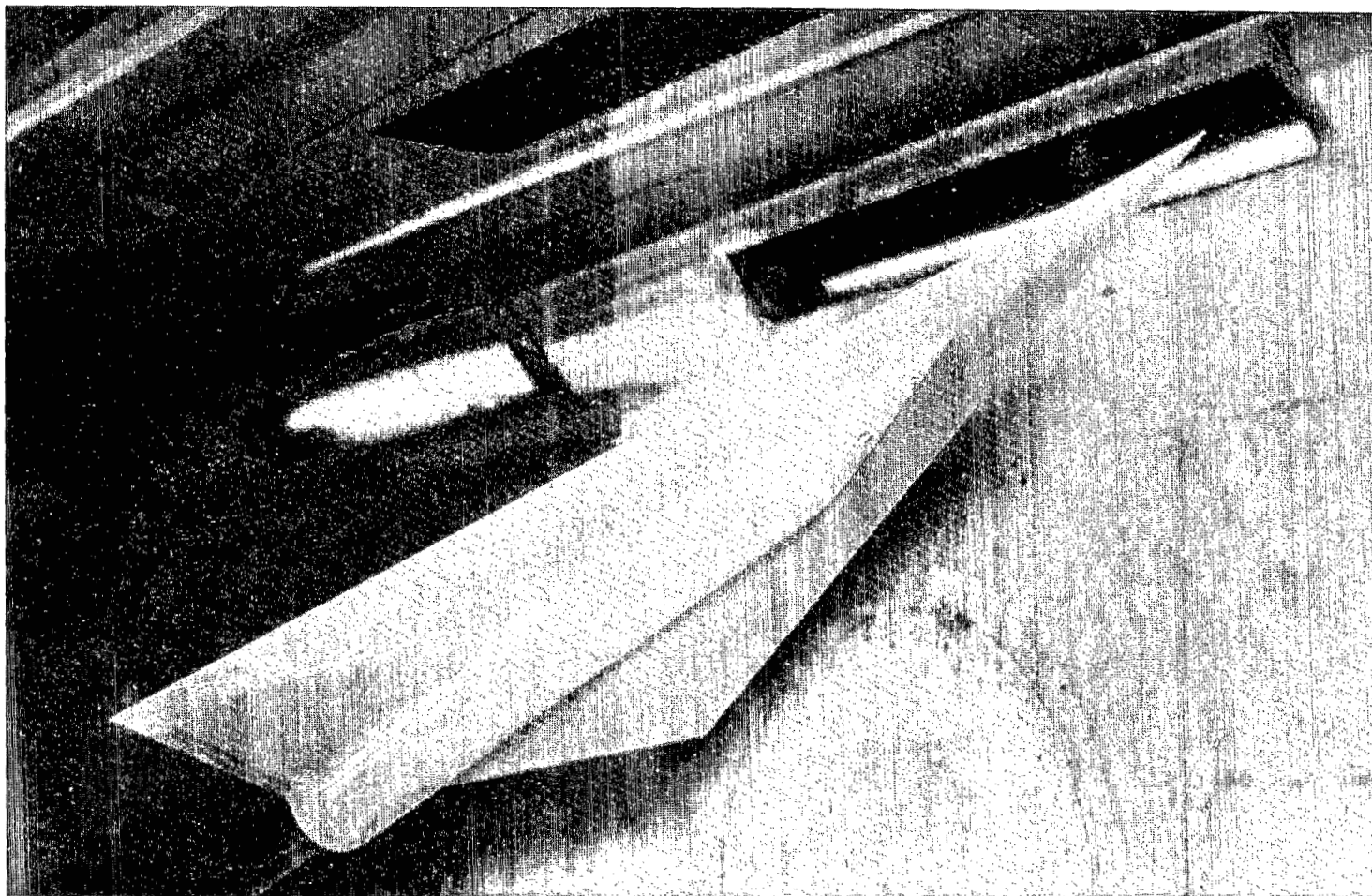
L-69-6022

(a) 37⁰ extended trailing-edge configuration.

Figure 2.- Typical model and components.
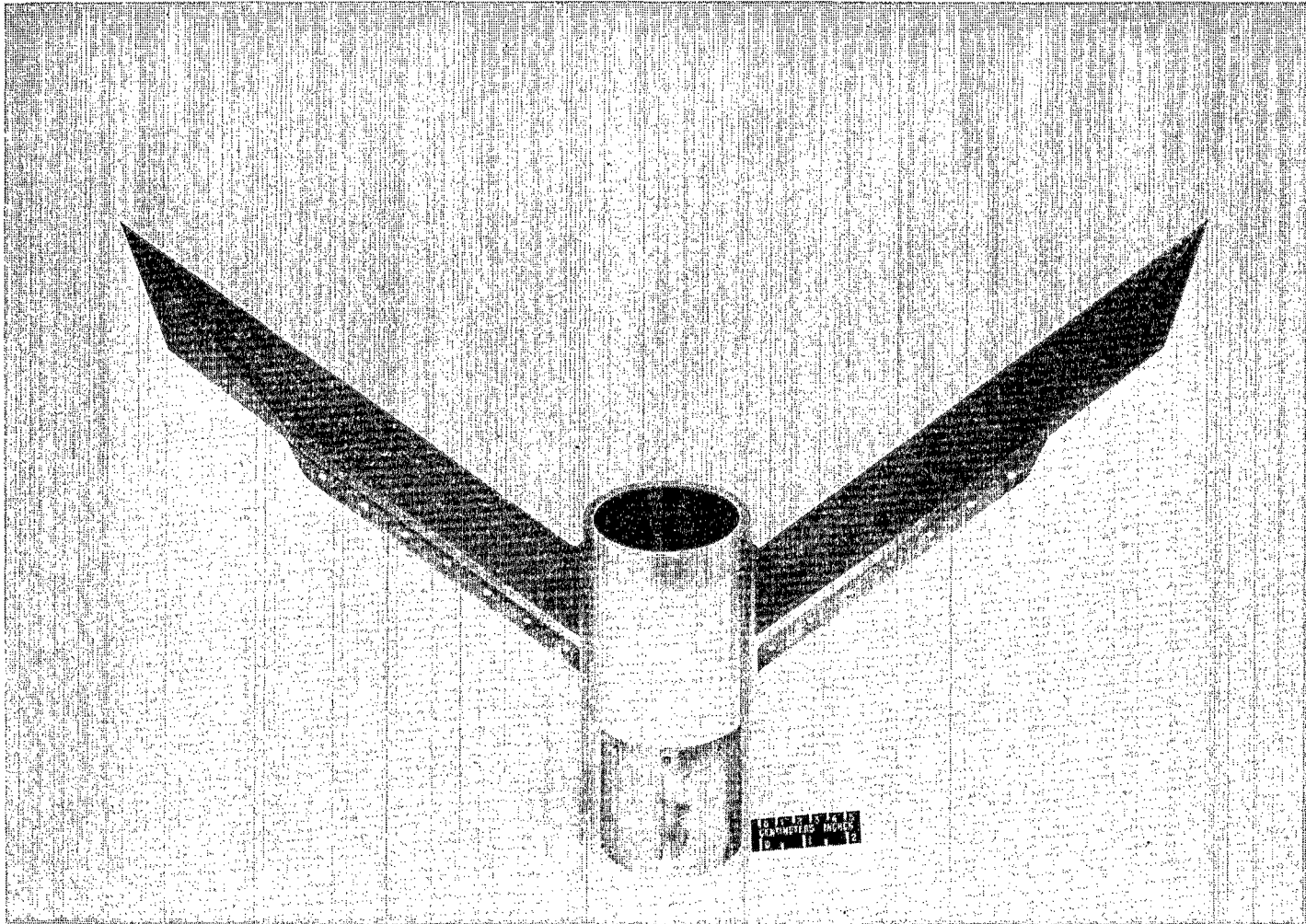
L-69-6055

(b) 37° recessed trailing-edge component.

Figure 2.- Continued.
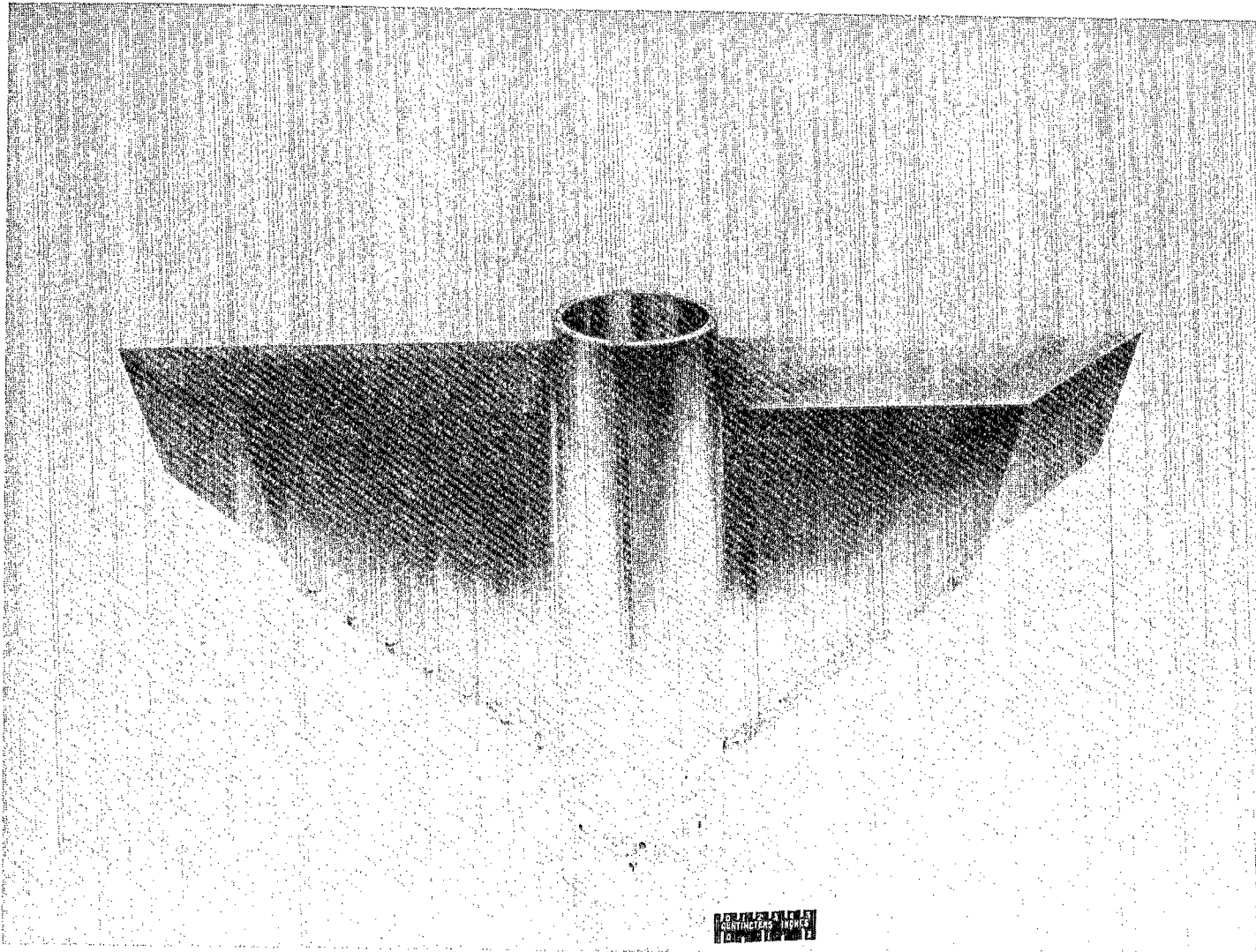
(c) 90$^{\text{O}}$ trailing-edge component.

Figure 2.- Concluded.

L-69-6054
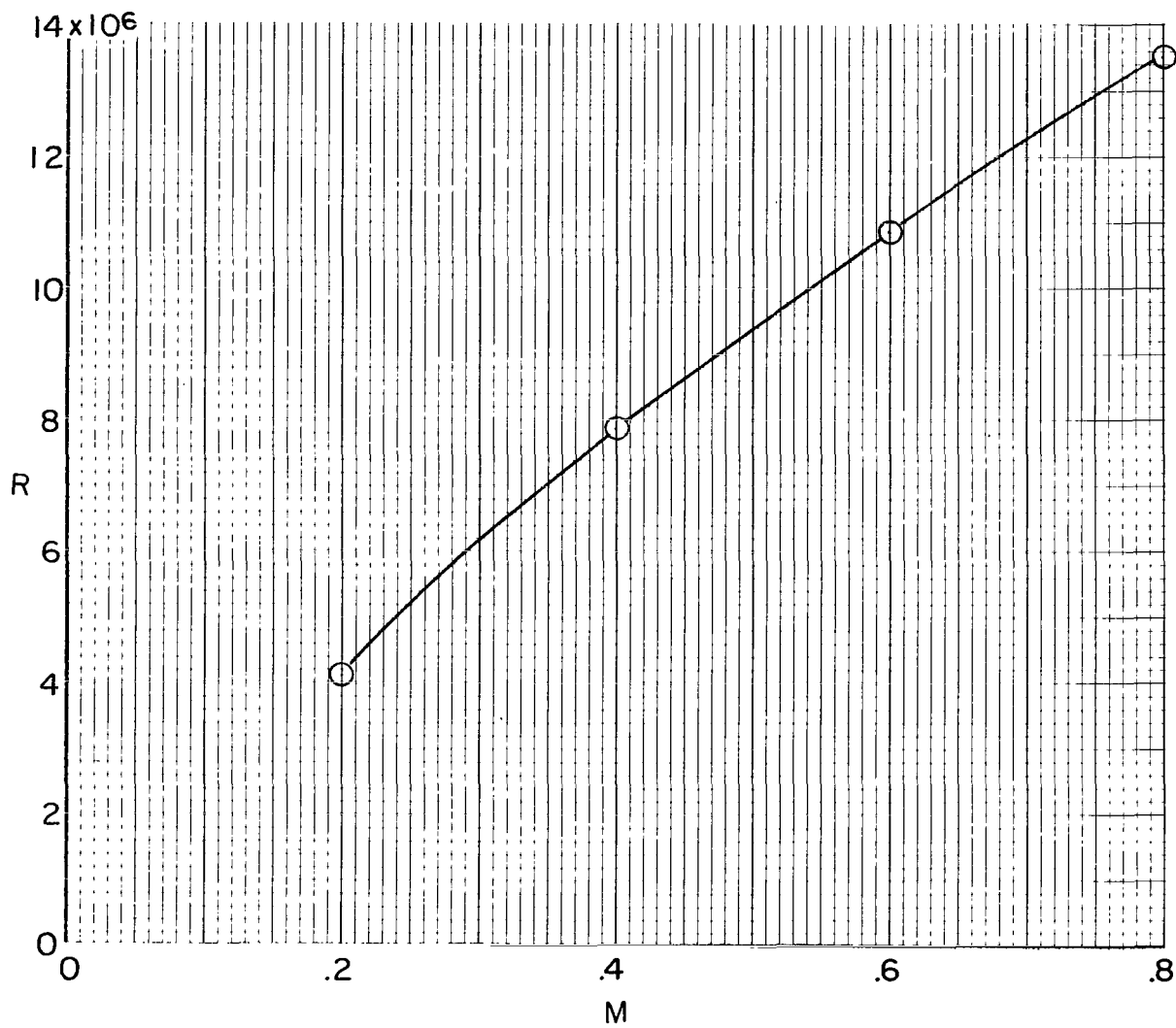
Figure 3.- Variation of Reynolds number with Mach number for average test conditions.
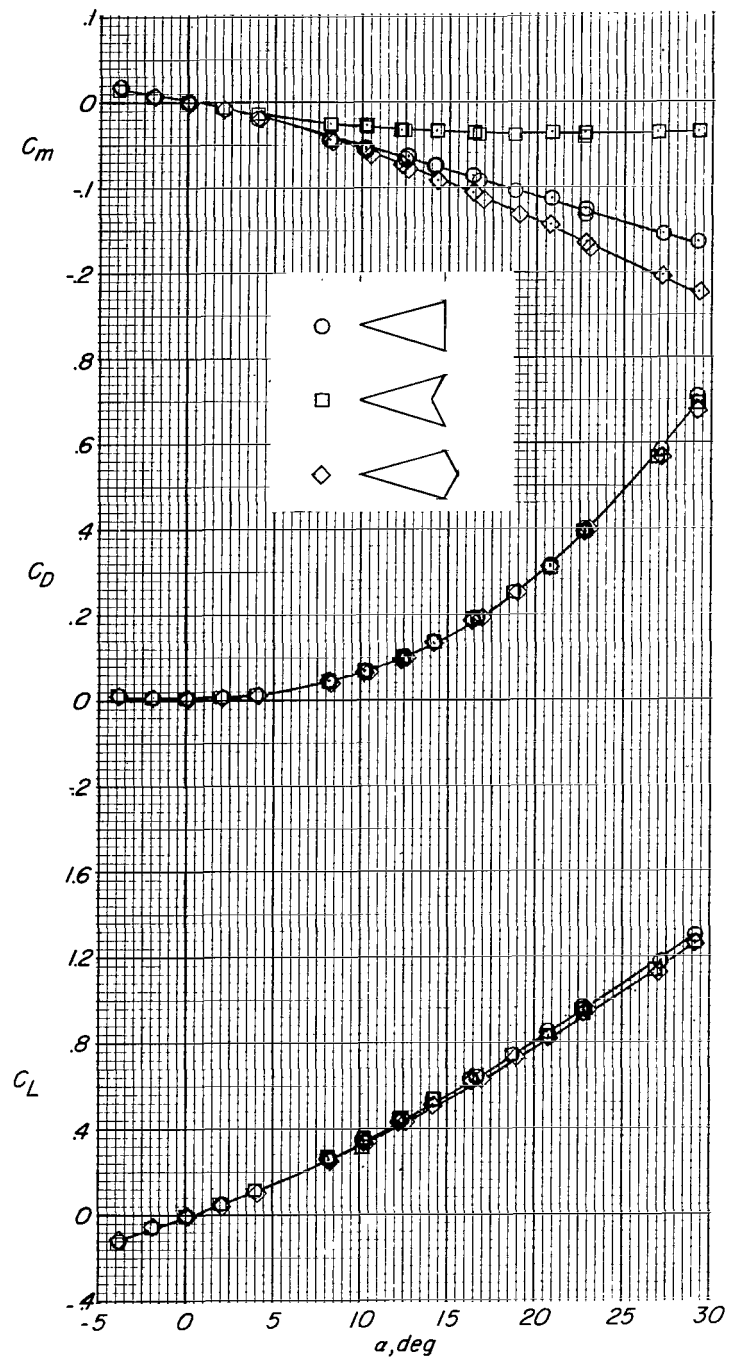
(a)   M = 0.2.

Figure 4.- Longitudinal aerodynamic characteristics at $\beta = 0^o$.
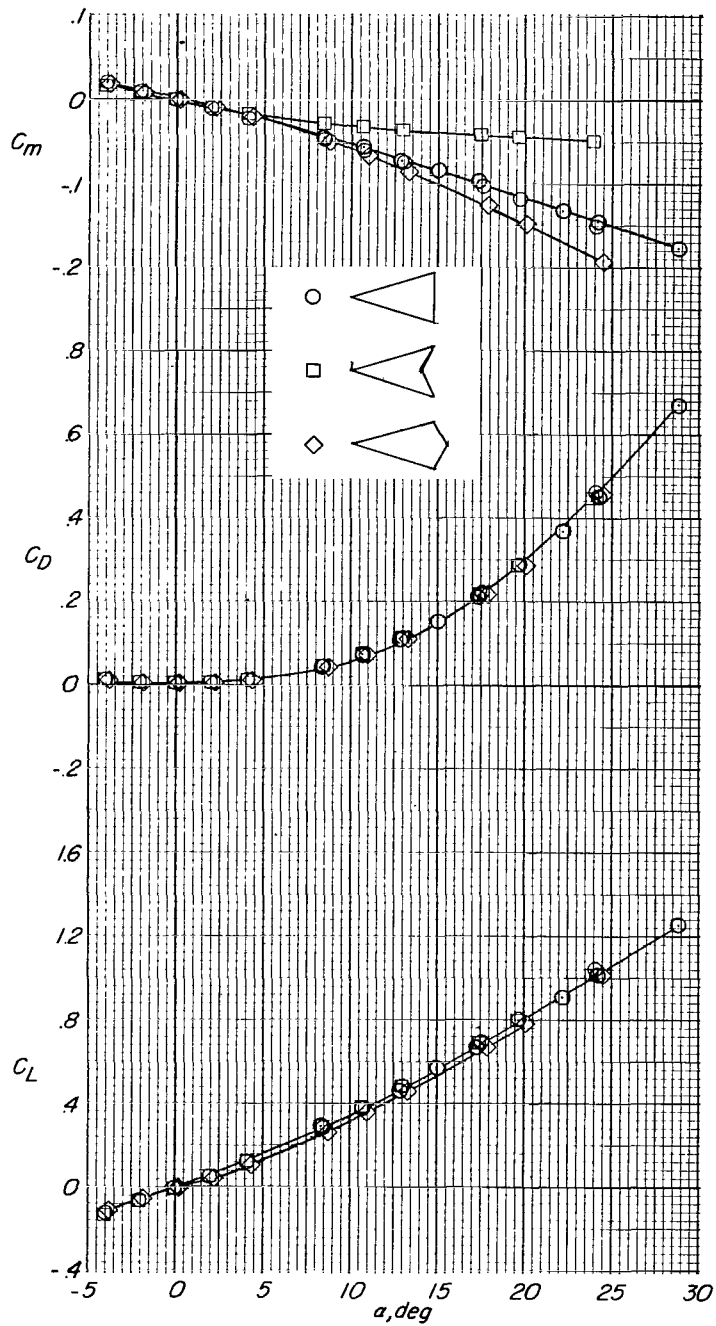
(b)   M = 0.4.

Figure 4.- Continued.
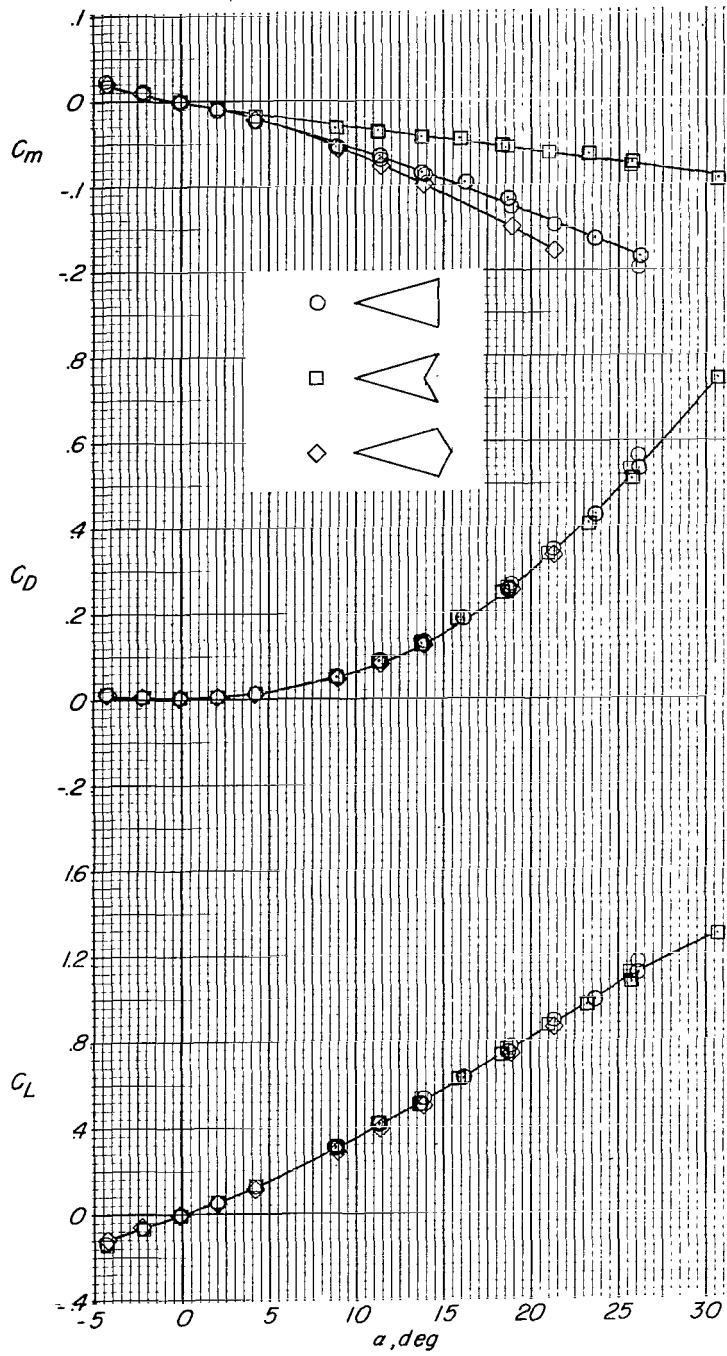
(c)   M = 0.6.

Figure 4.- Continued.
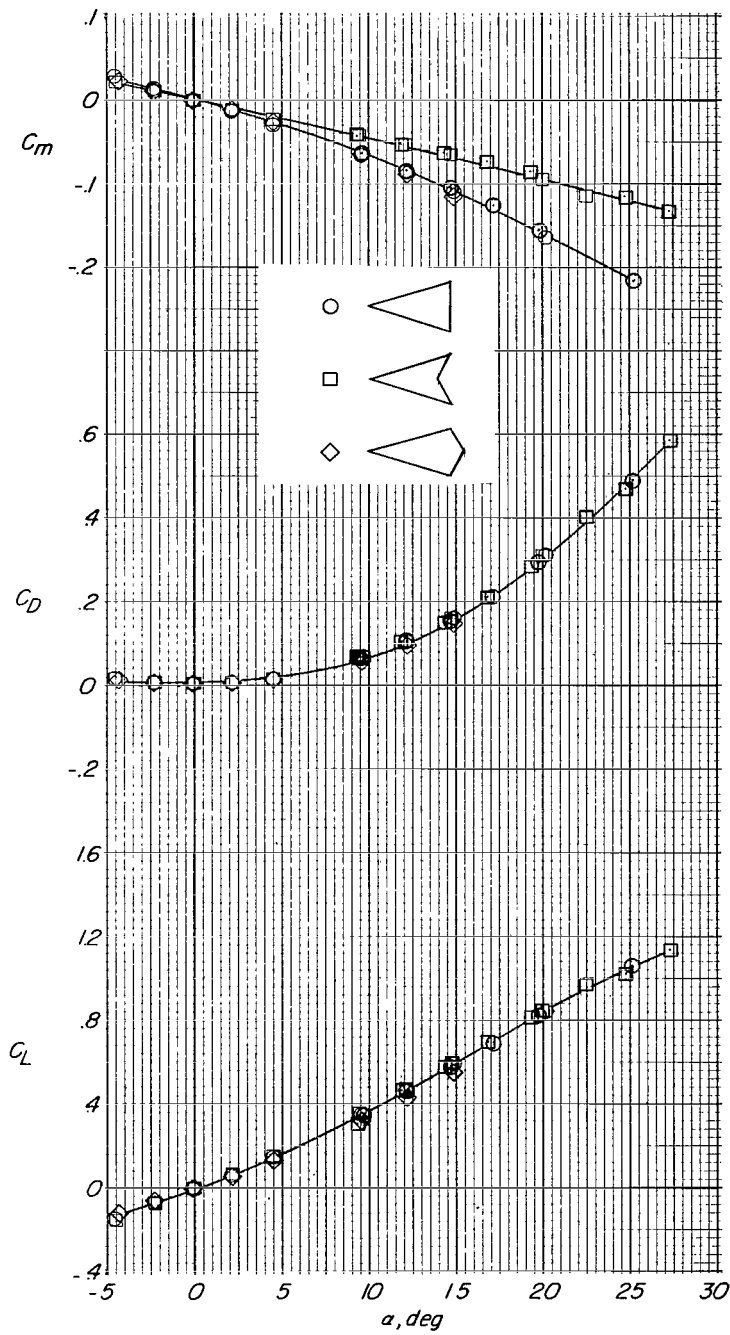
(d)   M = 0.8.

Figure 4.- Concluded.
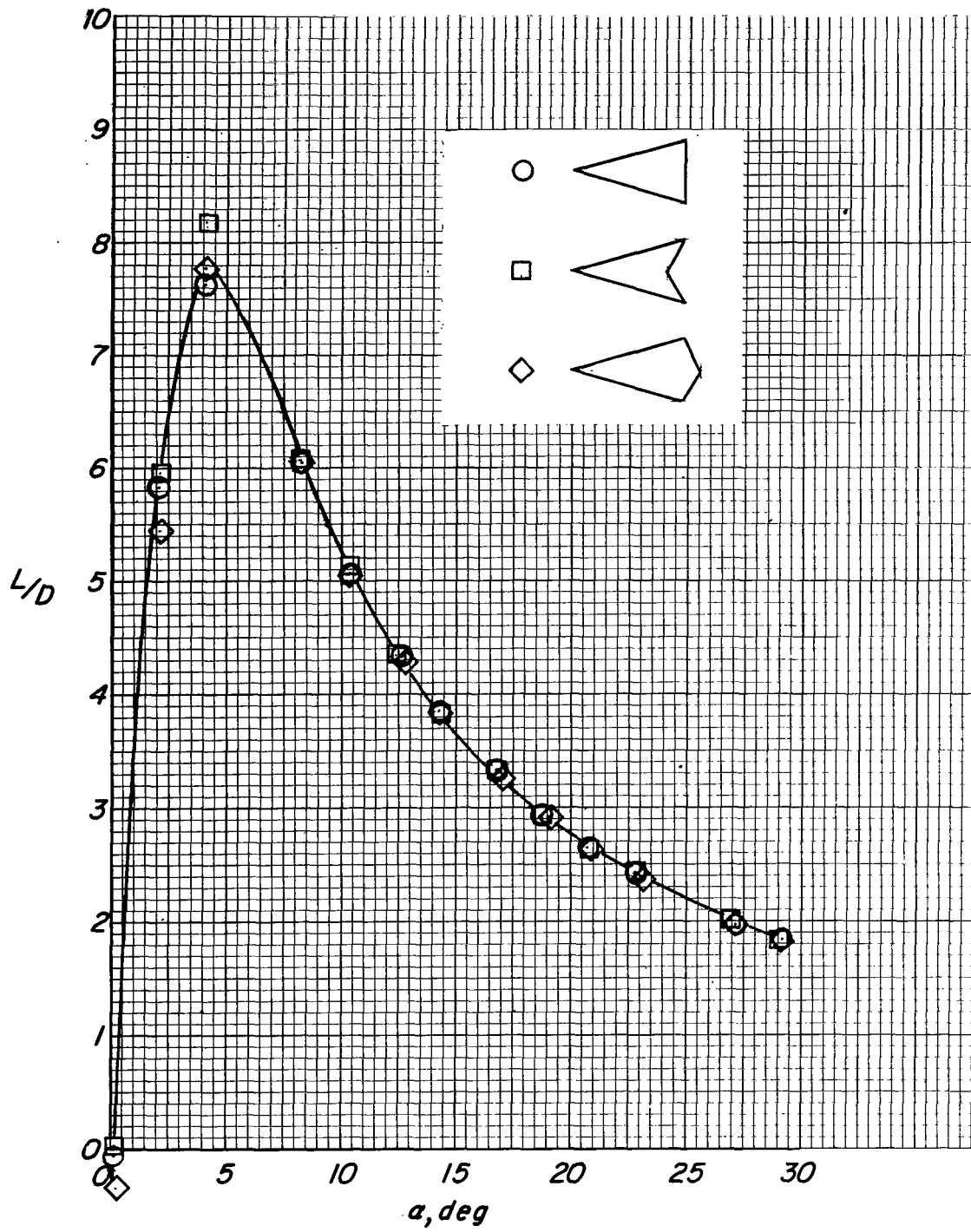
(a)   M = 0.2.

Figure 5.- Variation of   L/D   with α.
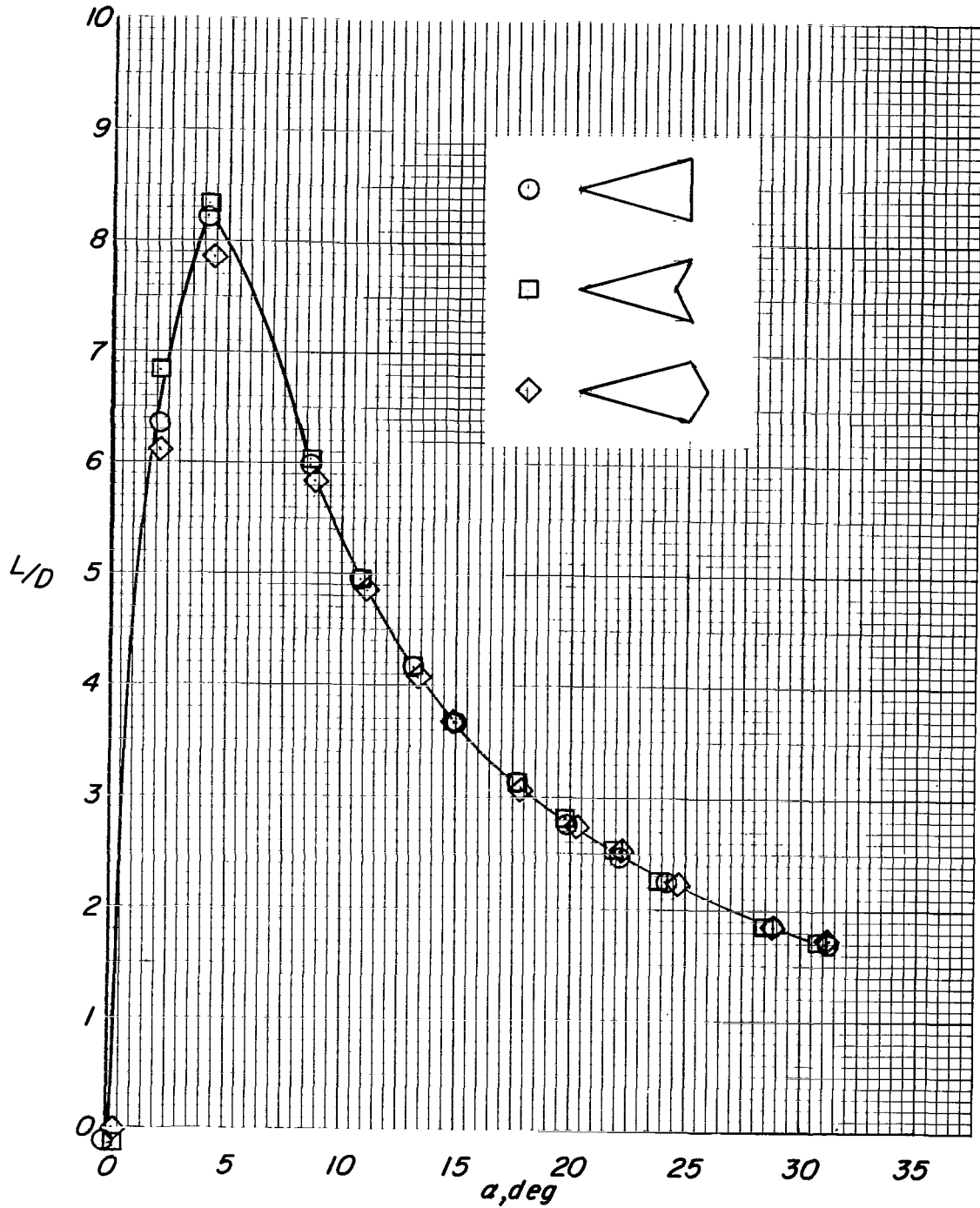
(b)   M = 0.4.

Figure 5.- Continued.
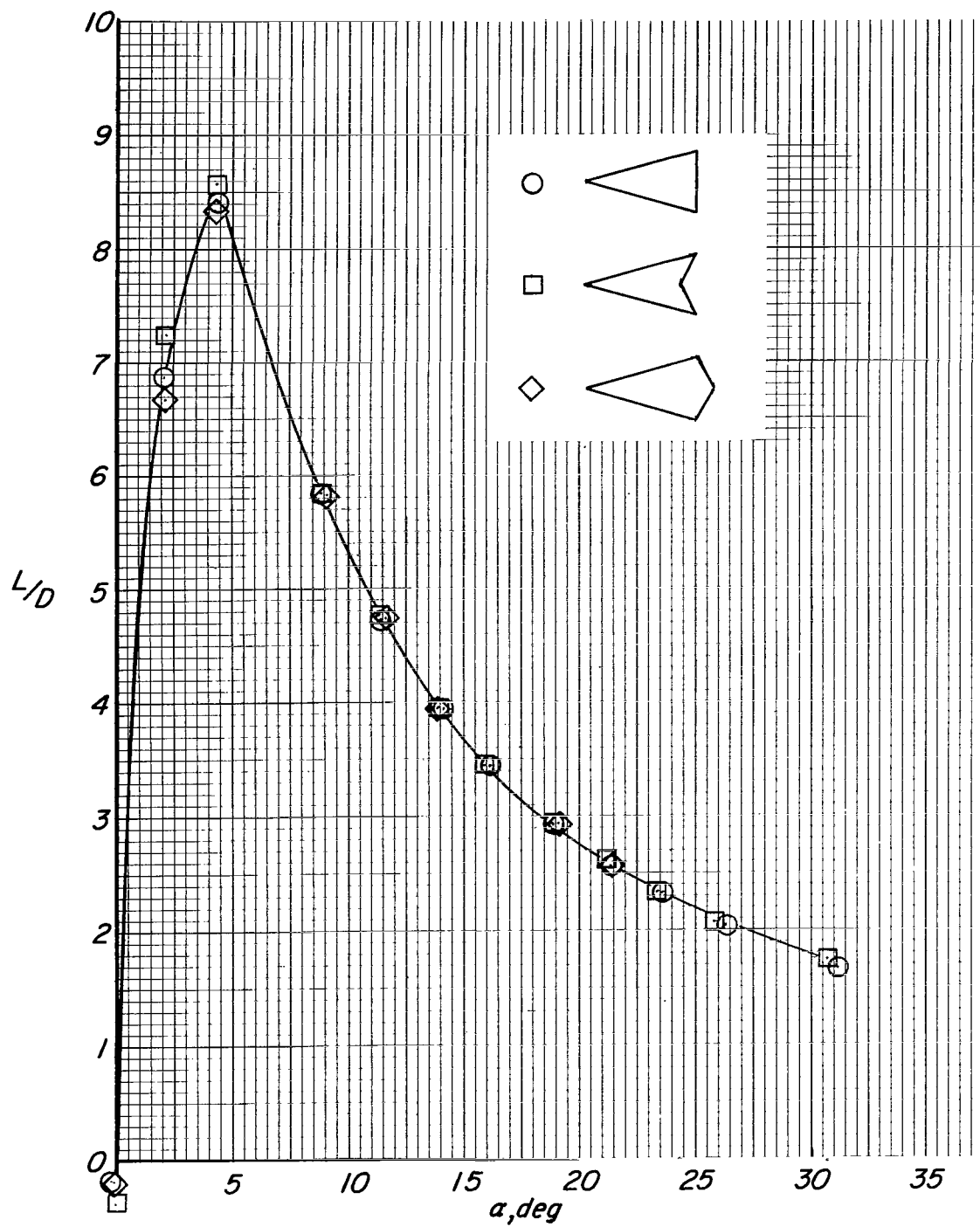
(c) M = 0.6.

Figure 5.- Continued.
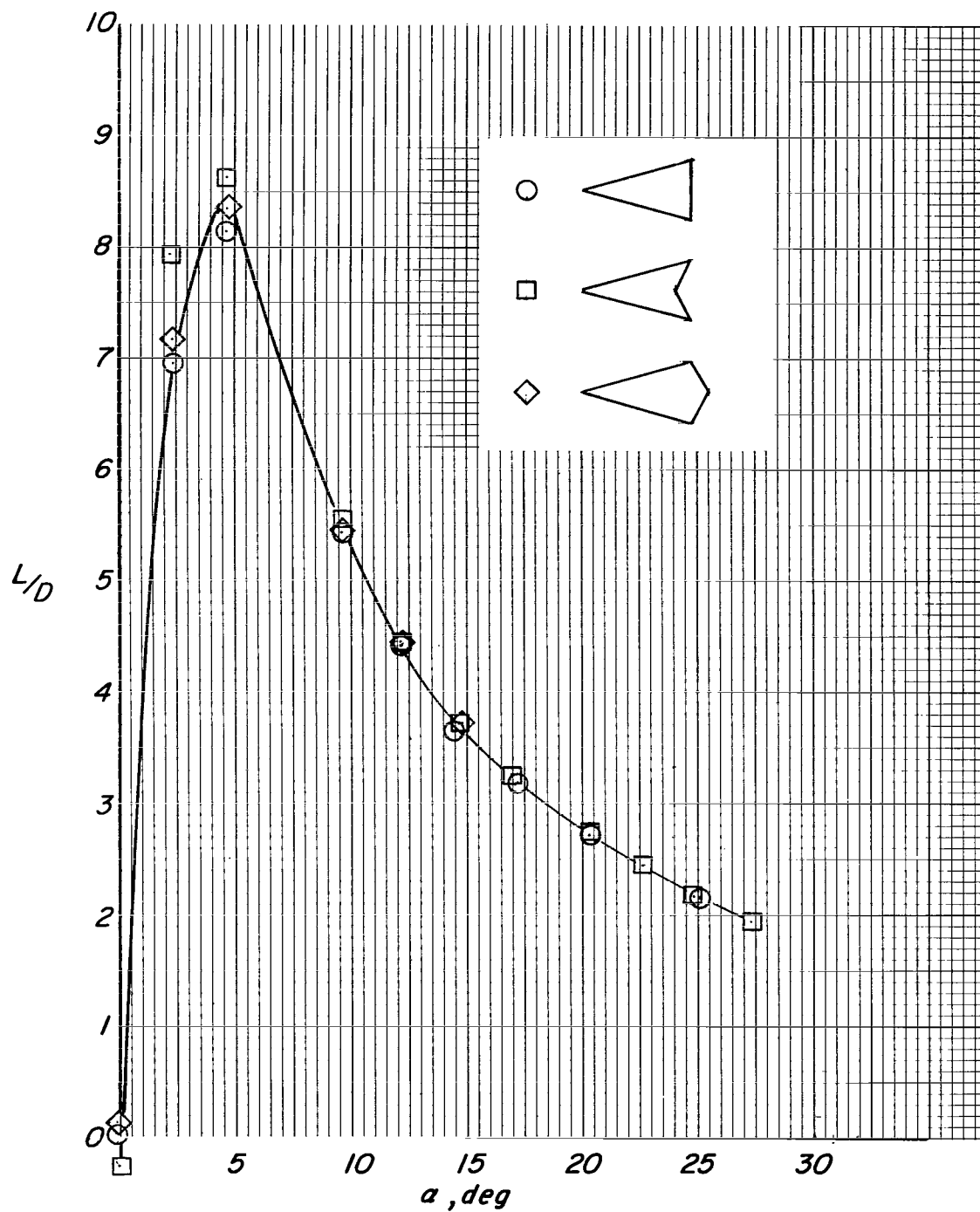
(d)   M = 0.8.

Figure 5.- Concluded.
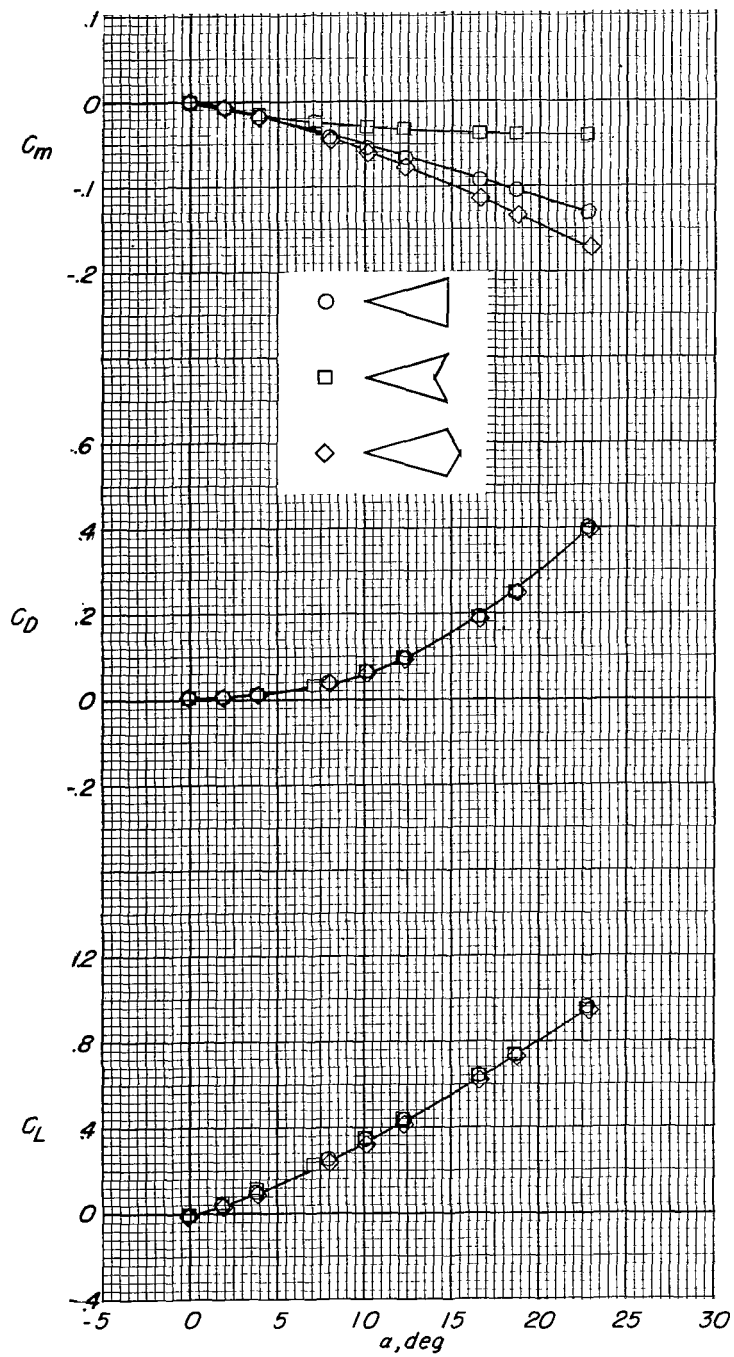
(a) M = 0.2.

Figure 6.- Longitudinal aerodynamic characteristics at $\beta = 4^{o}$.
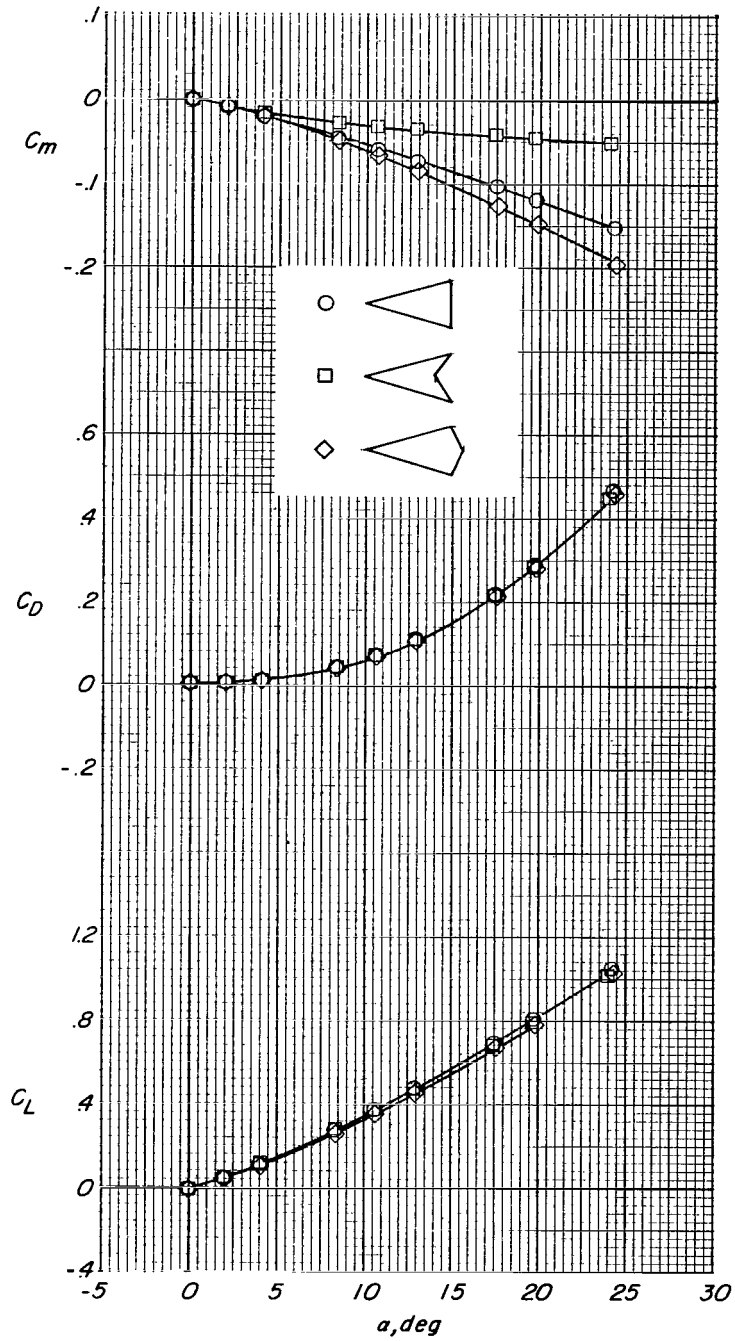
(b)   M = 0.4.

Figure 6.- Continued.
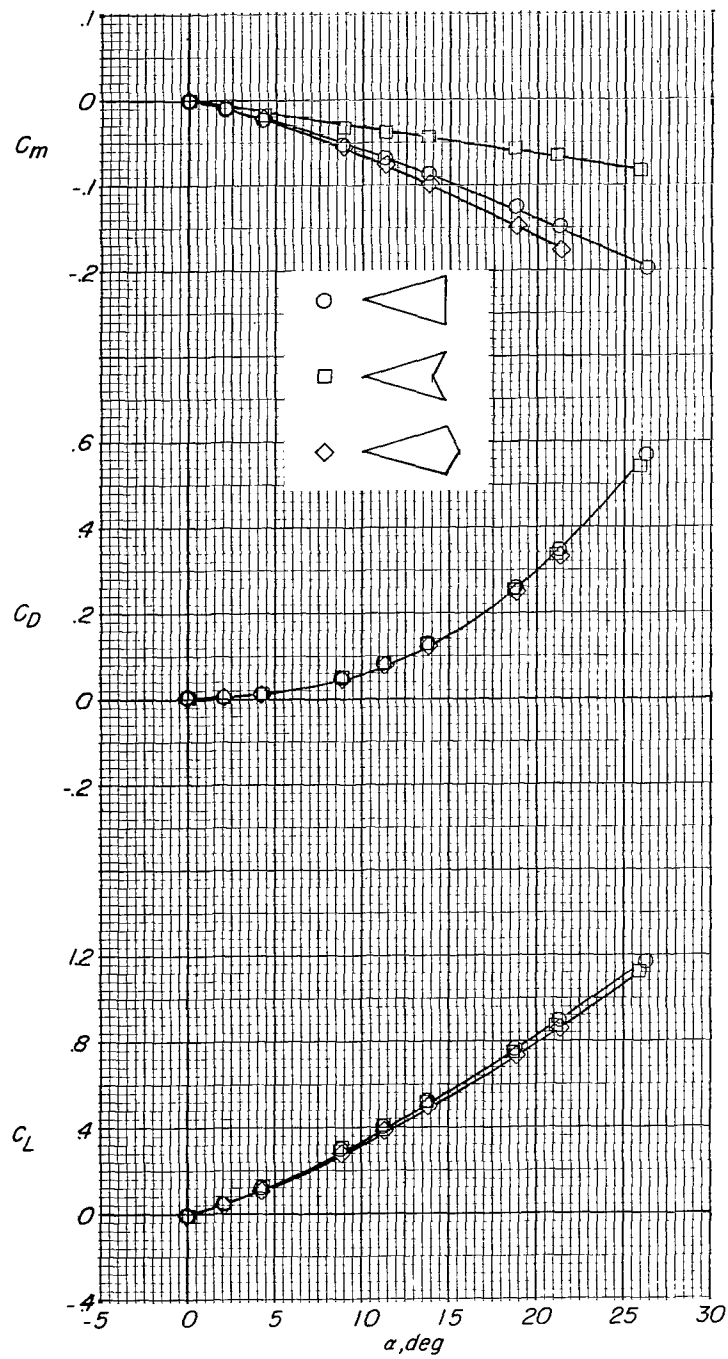
(c)   M = 0.6.

Figure 6.- Continued.
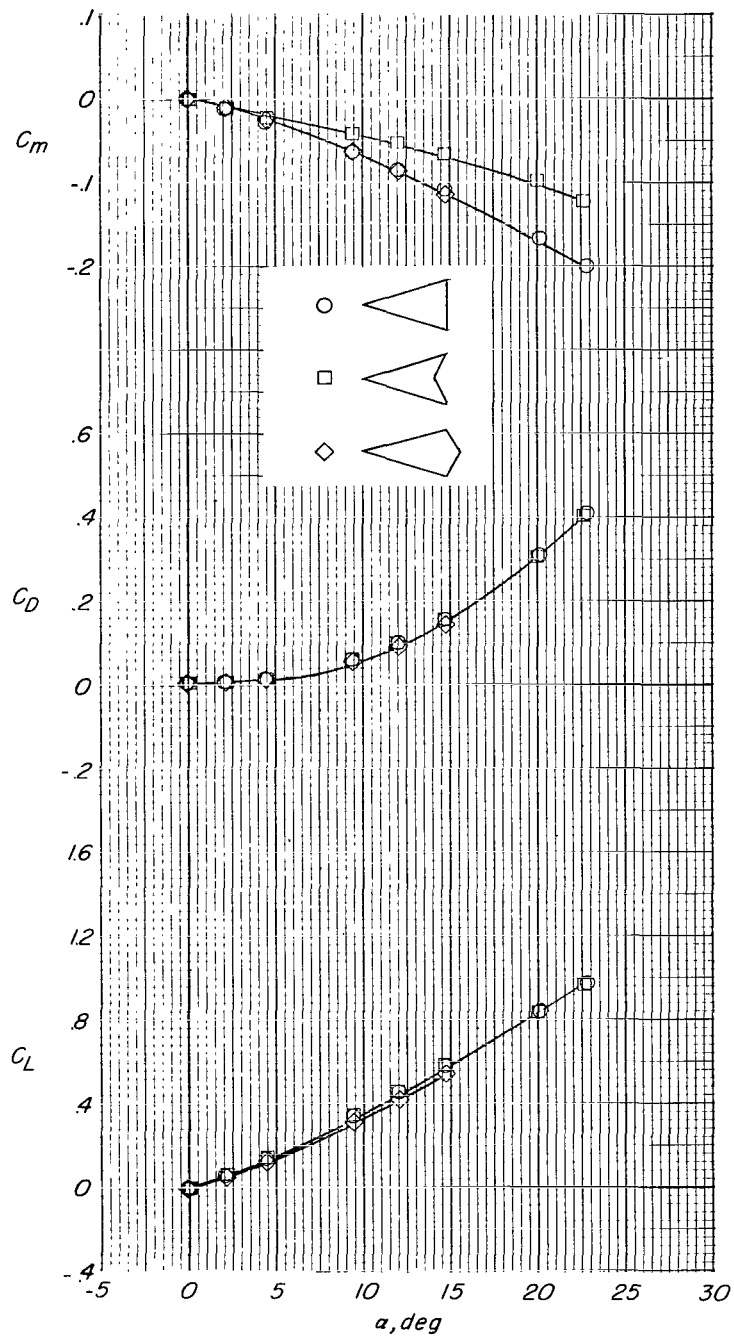
(d) M = 0.8.

Figure 6.- Concluded.
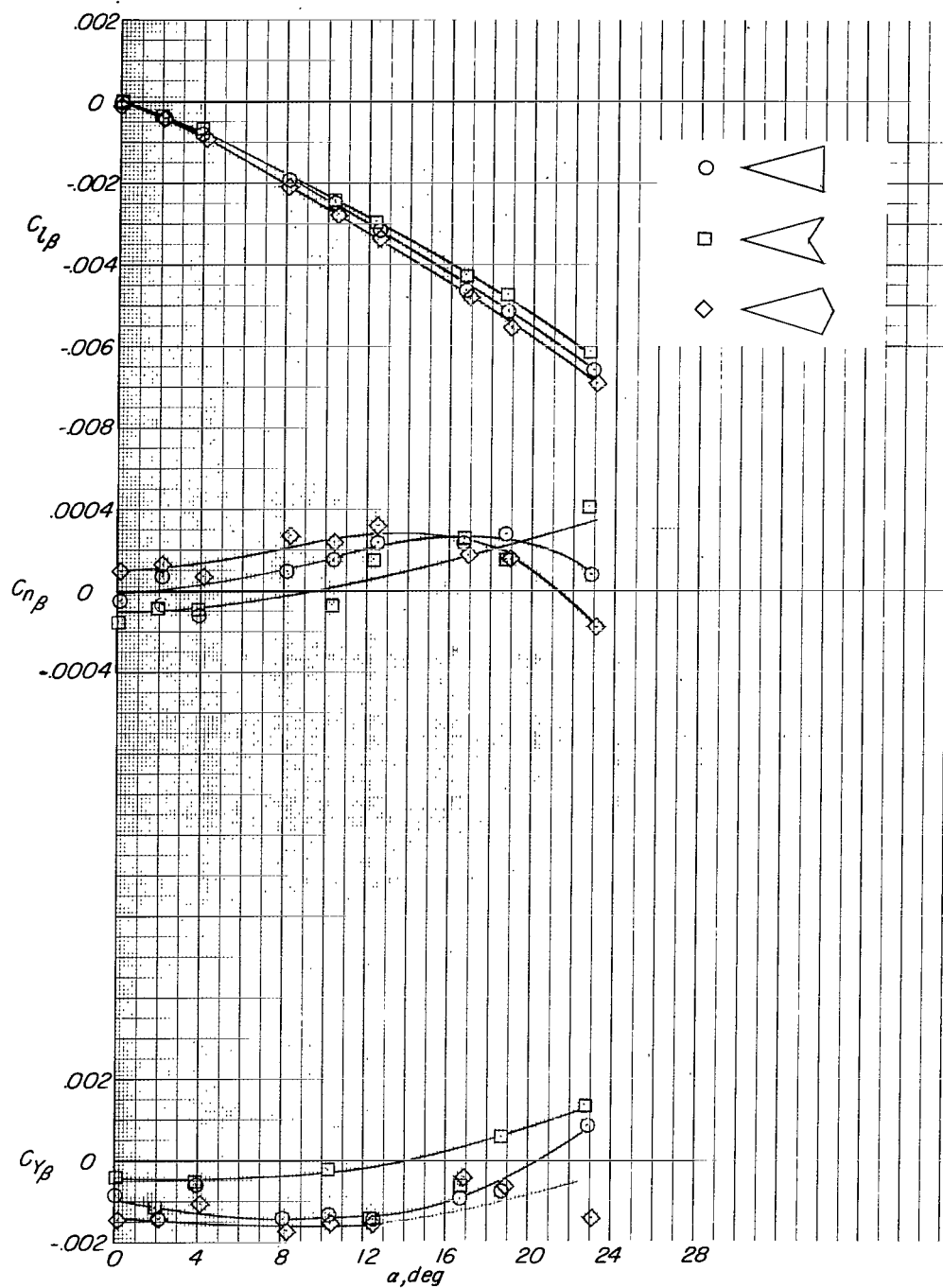
(a) M = 0.2.

Figure 7.- Variation of lateral stability derivatives with angle of attack at $\beta = 4^O$.
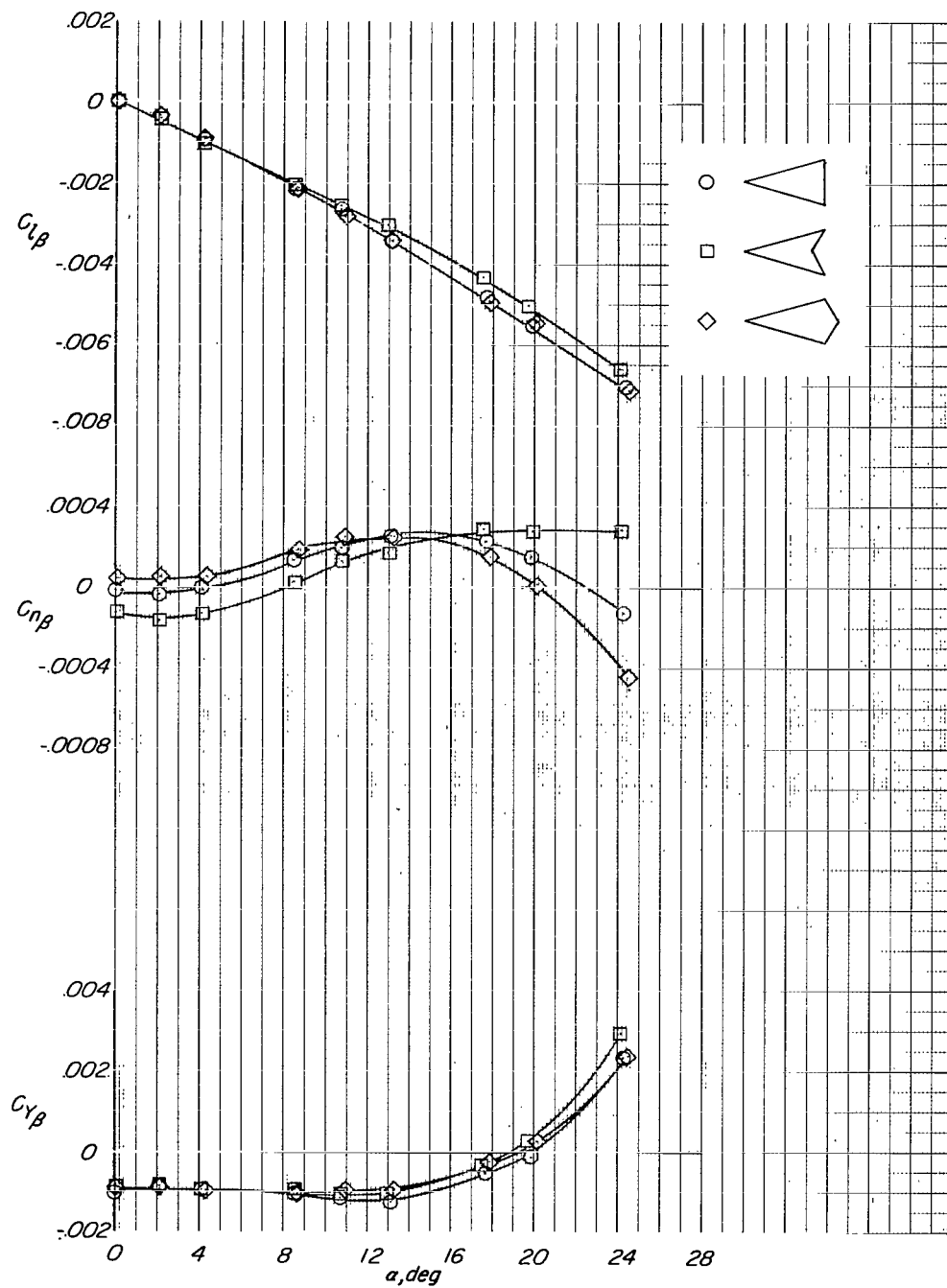
(b) M = 0.4.

Figure 7.- Continued.
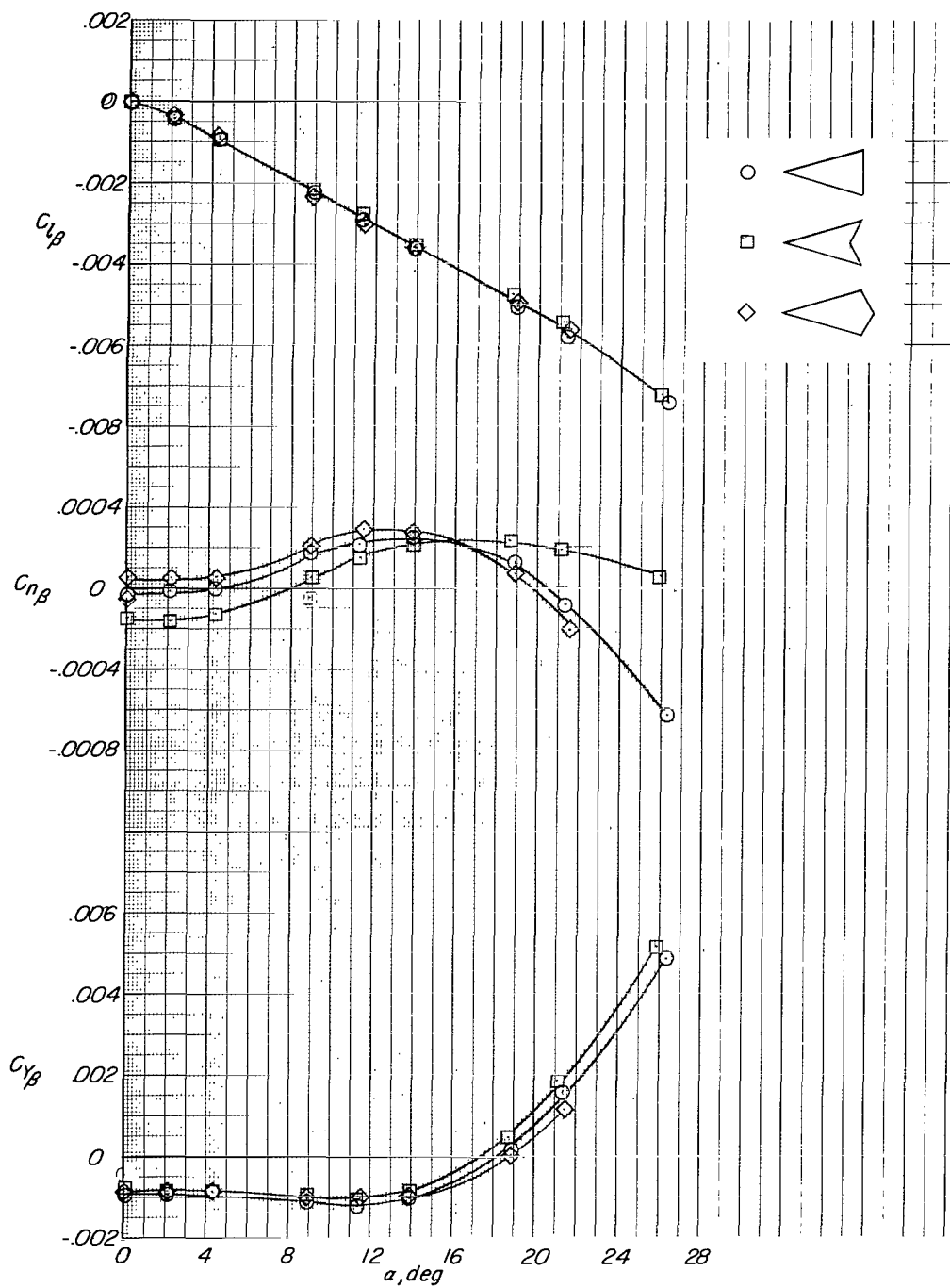
(c)   M = 0.6.

Figure 7.- Continued.
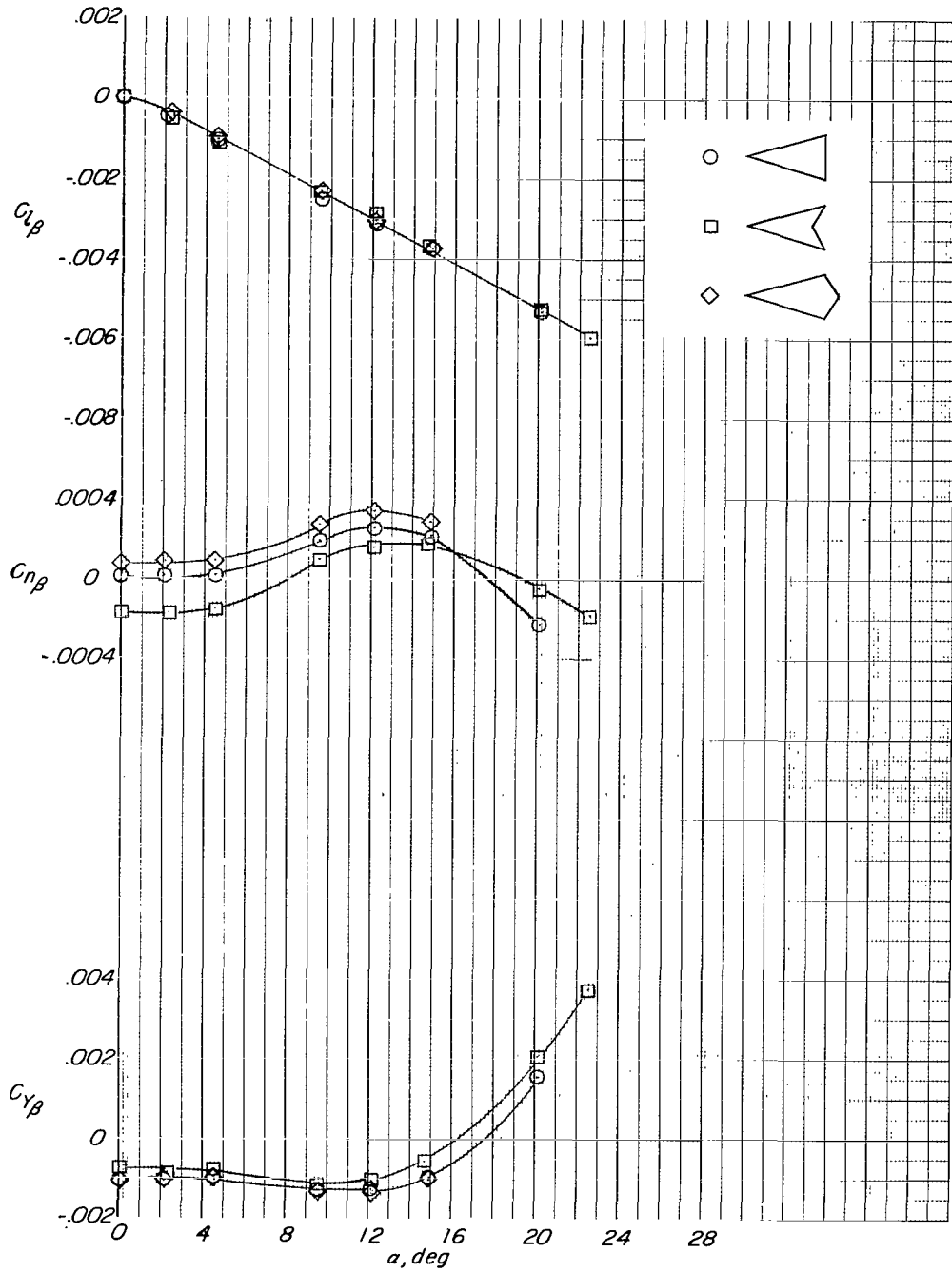
(d)   M = 0.8.

Figure 7.- Concluded.

(a) $\alpha = 4^{o}$.
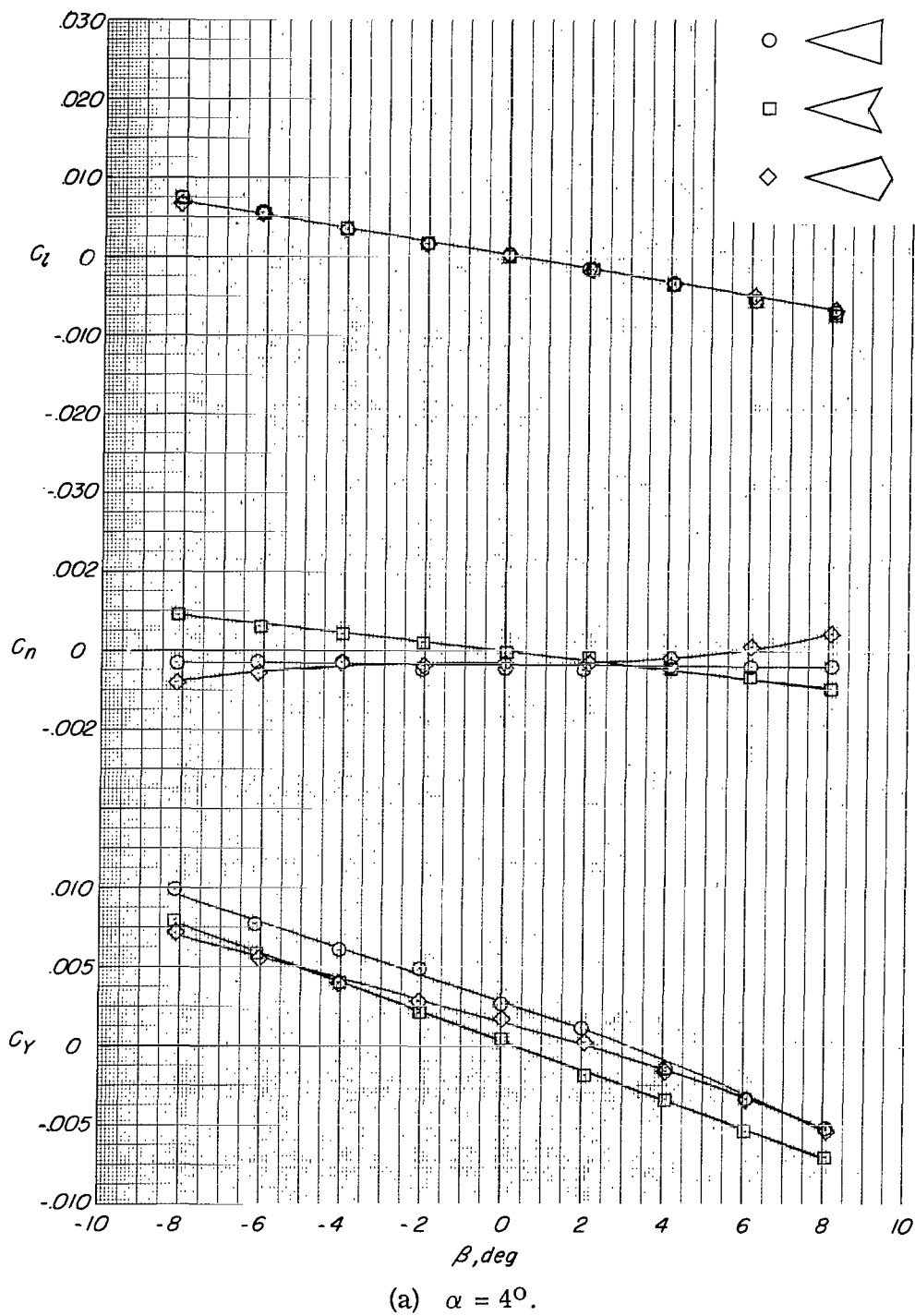
Figure 8.- Static lateral aerodynamic characteristics at angle of attack. M = 0.4.
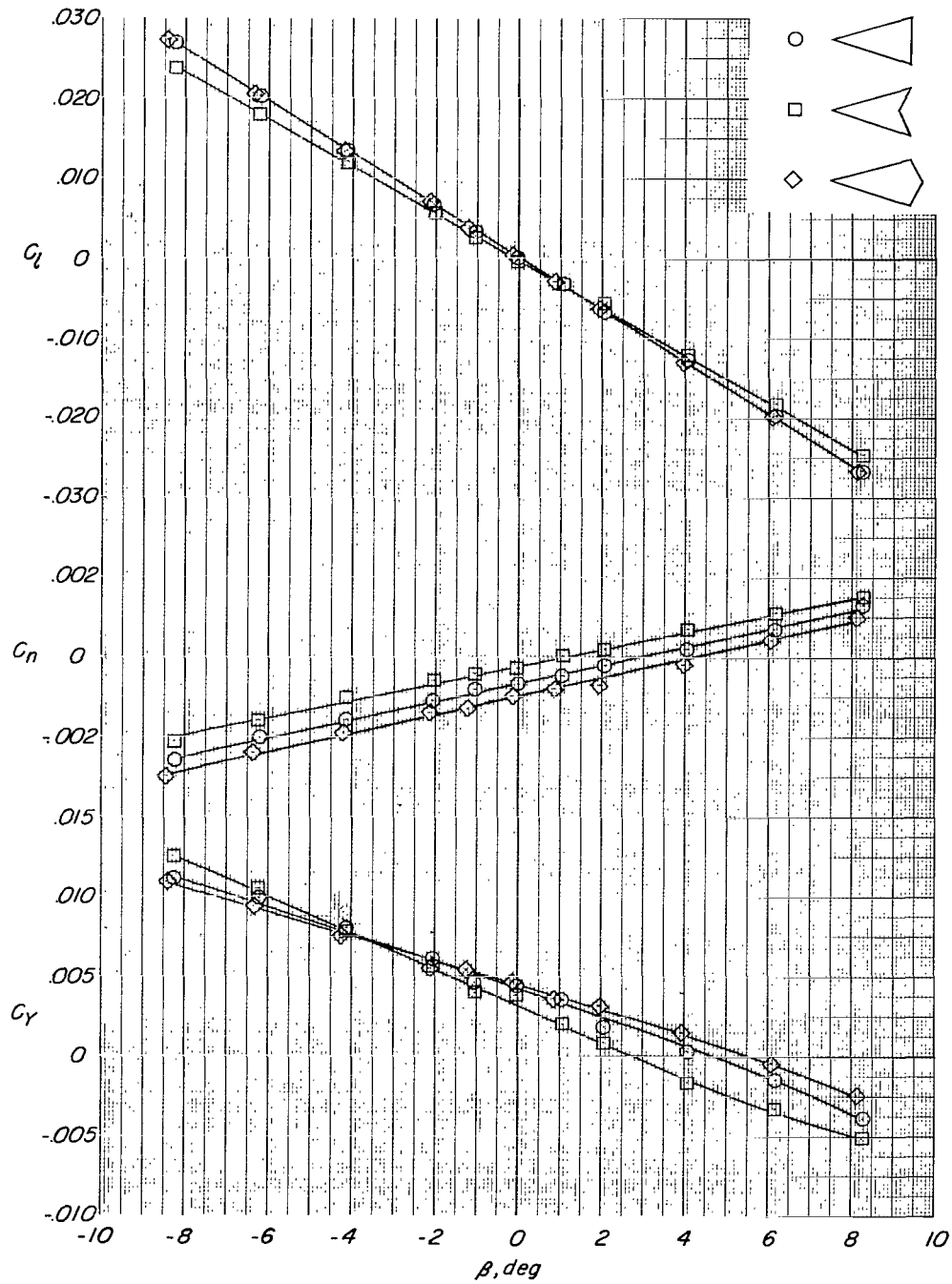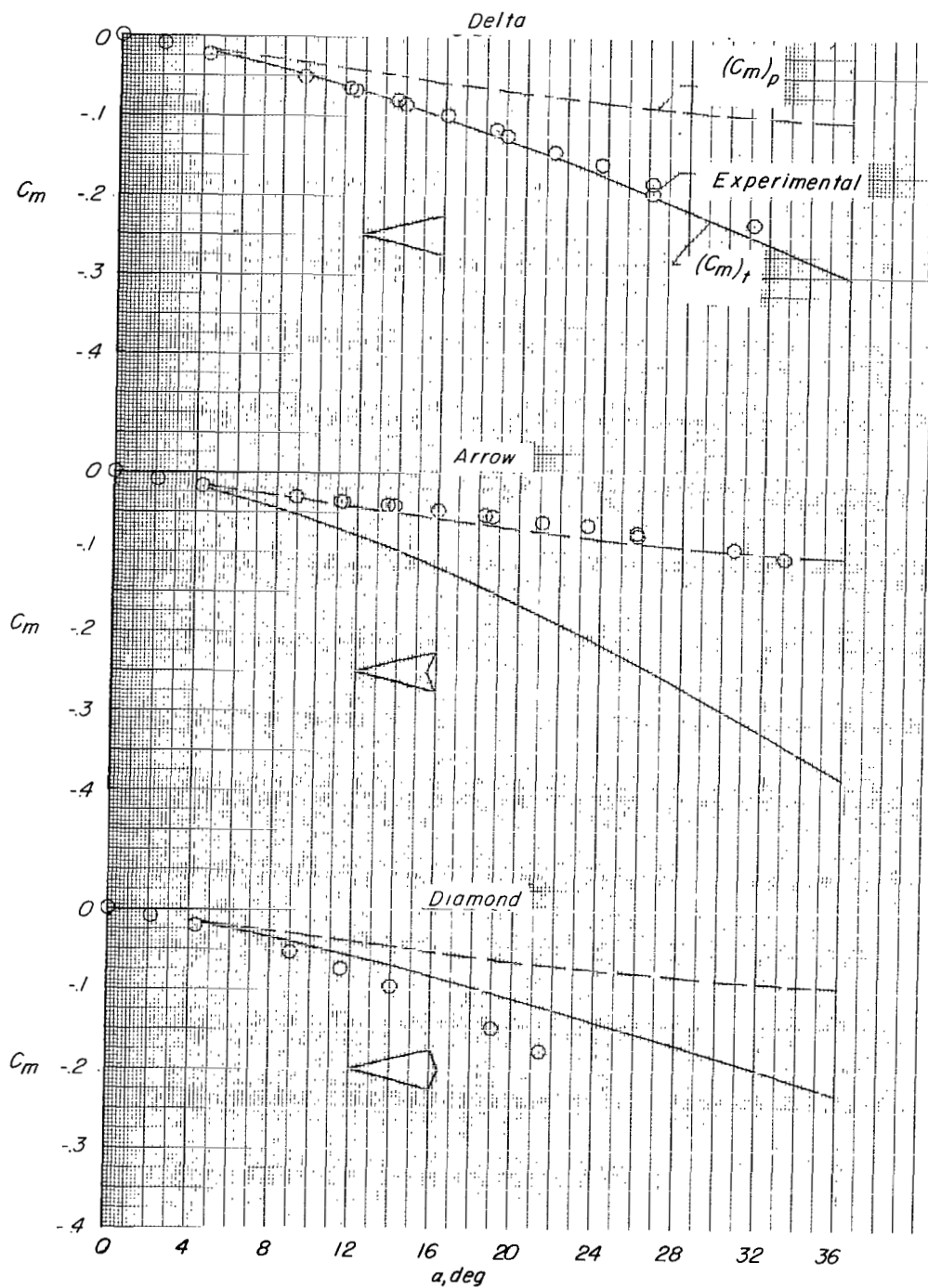
(b) $\alpha = 12°$.

Figure 8.- Concluded.
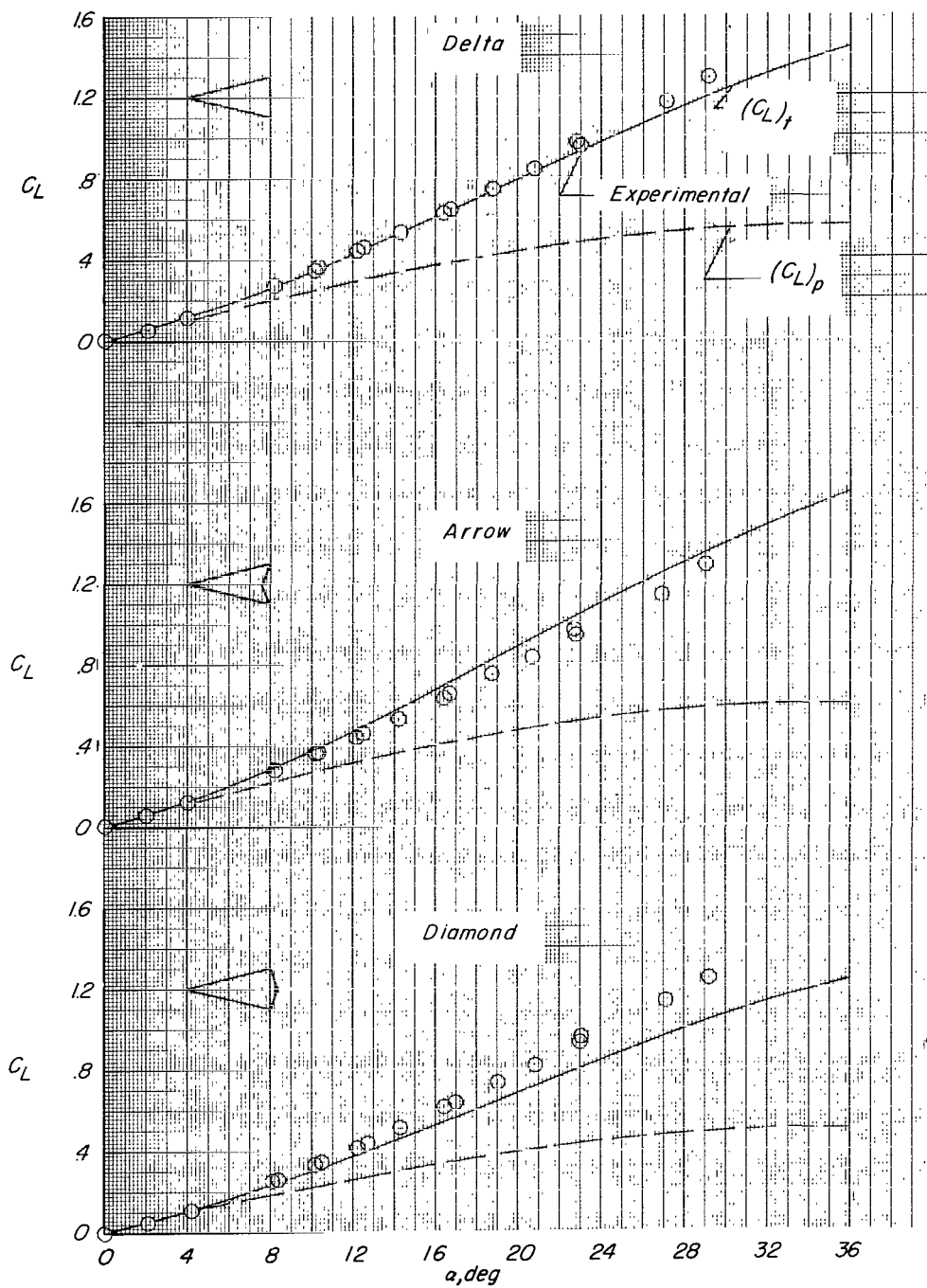
(a) M = 0.2.

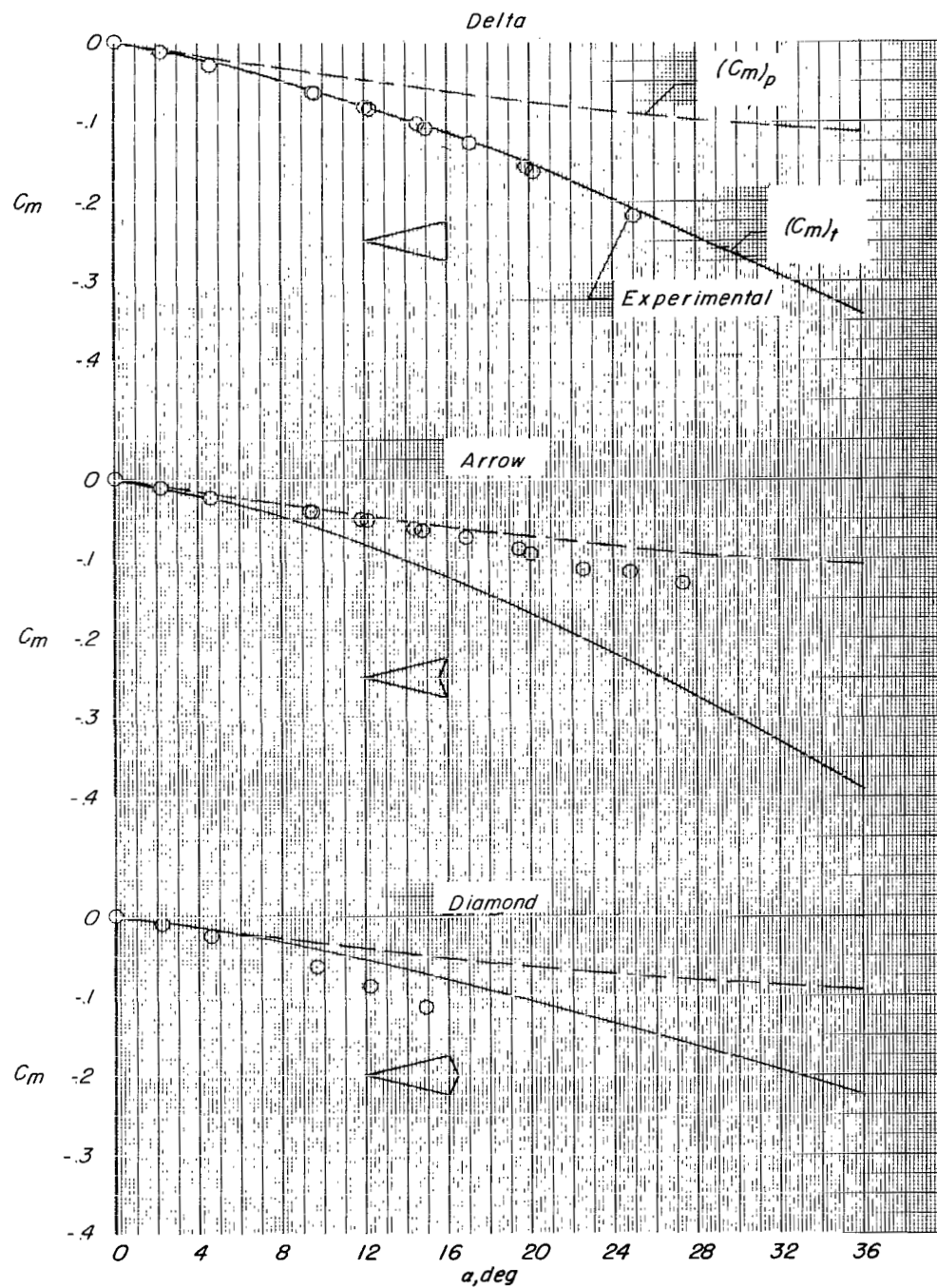Figure 9.- Theoretical and experimental lift characteristics.
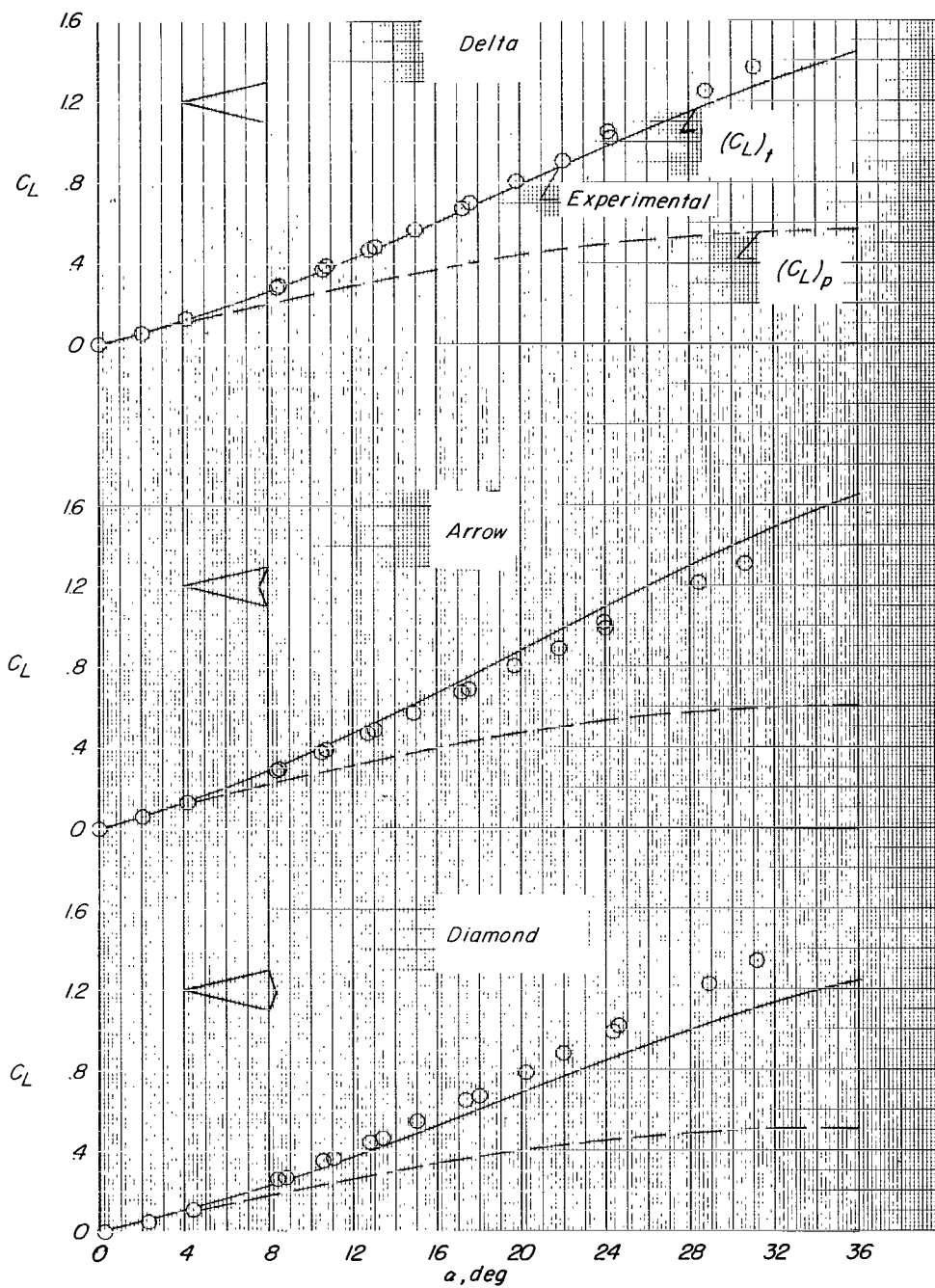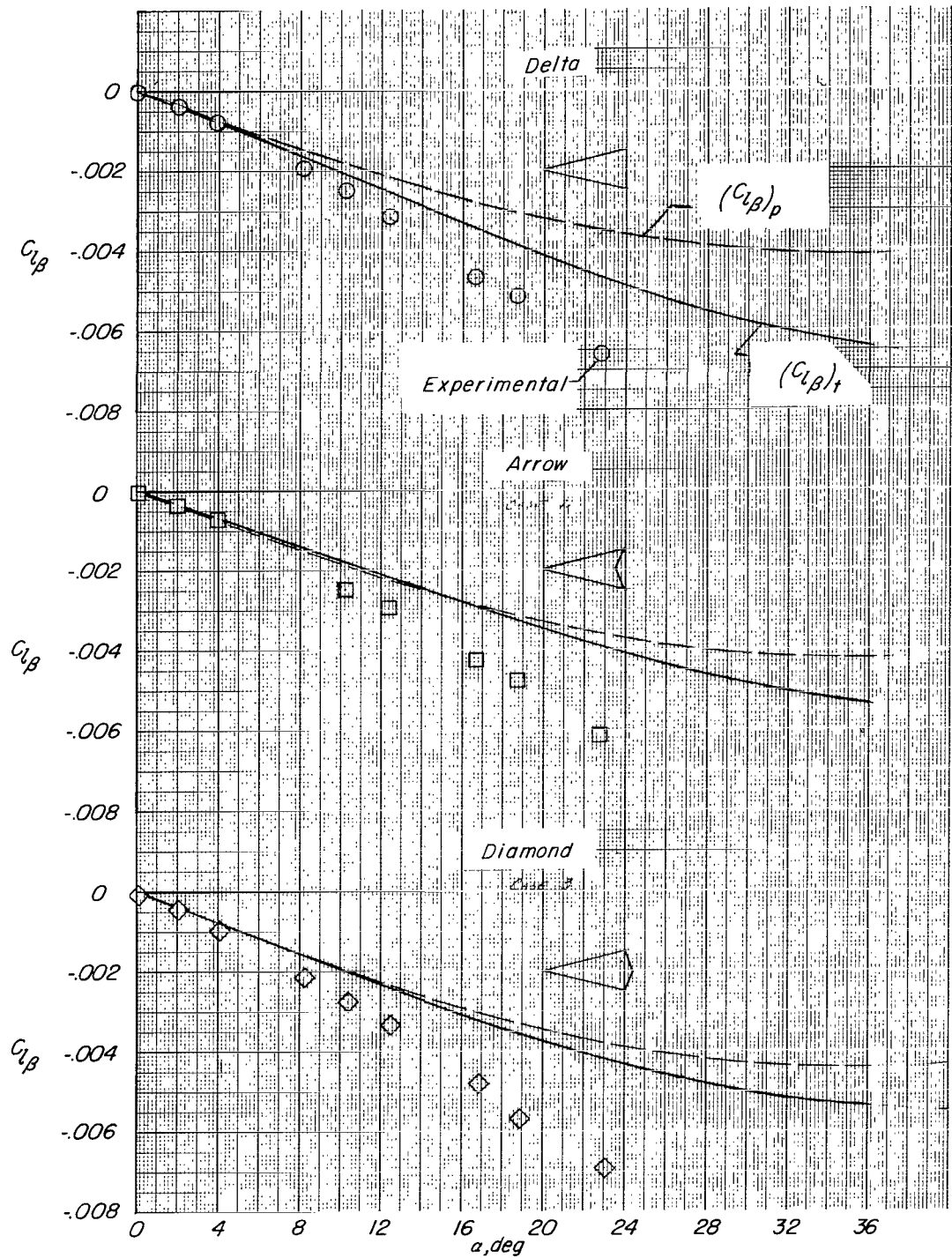
(b) M = 0.4.

Figure 9.- Continued.
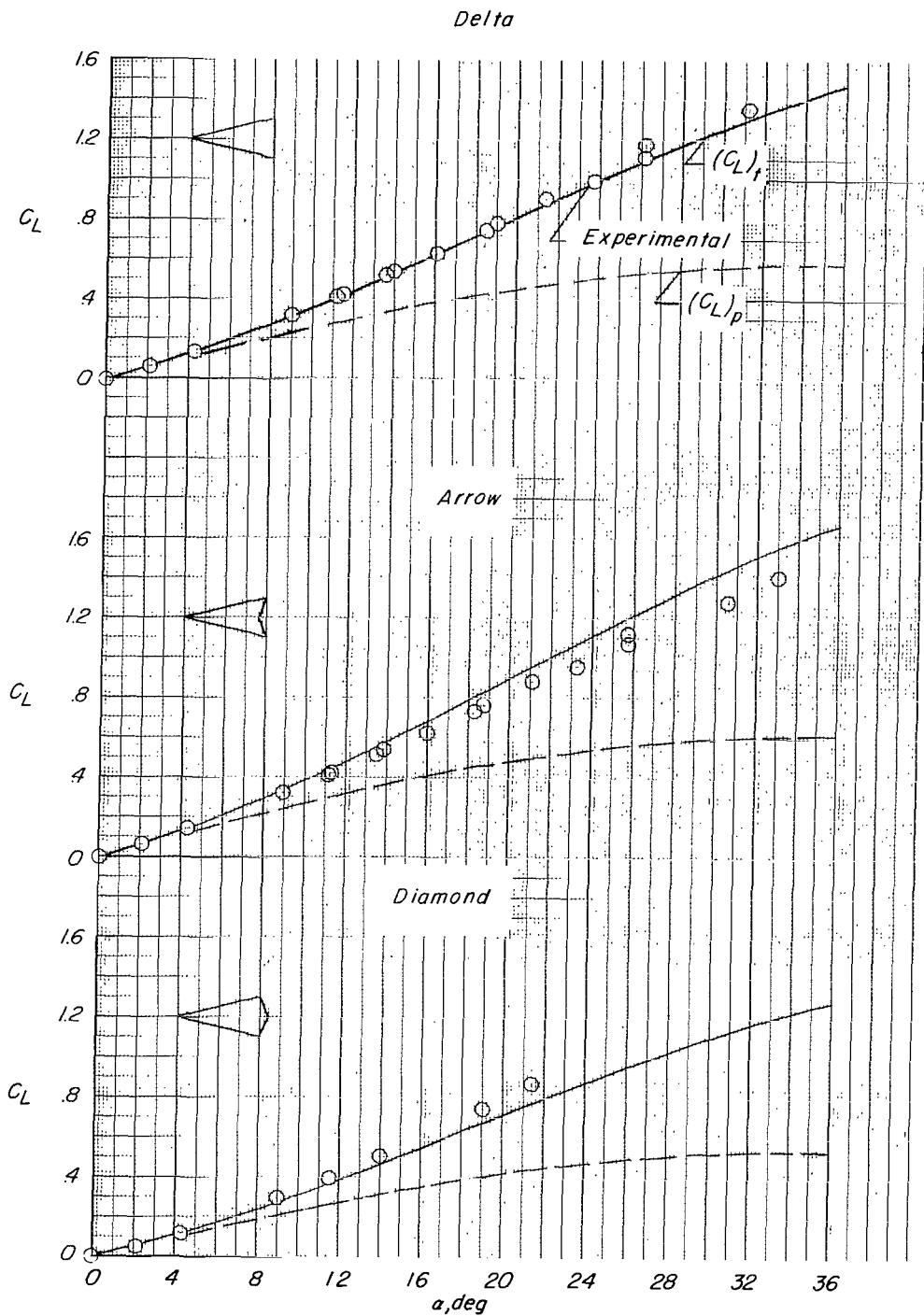
(c) M = 0.6.

Figure 9.- Continued.
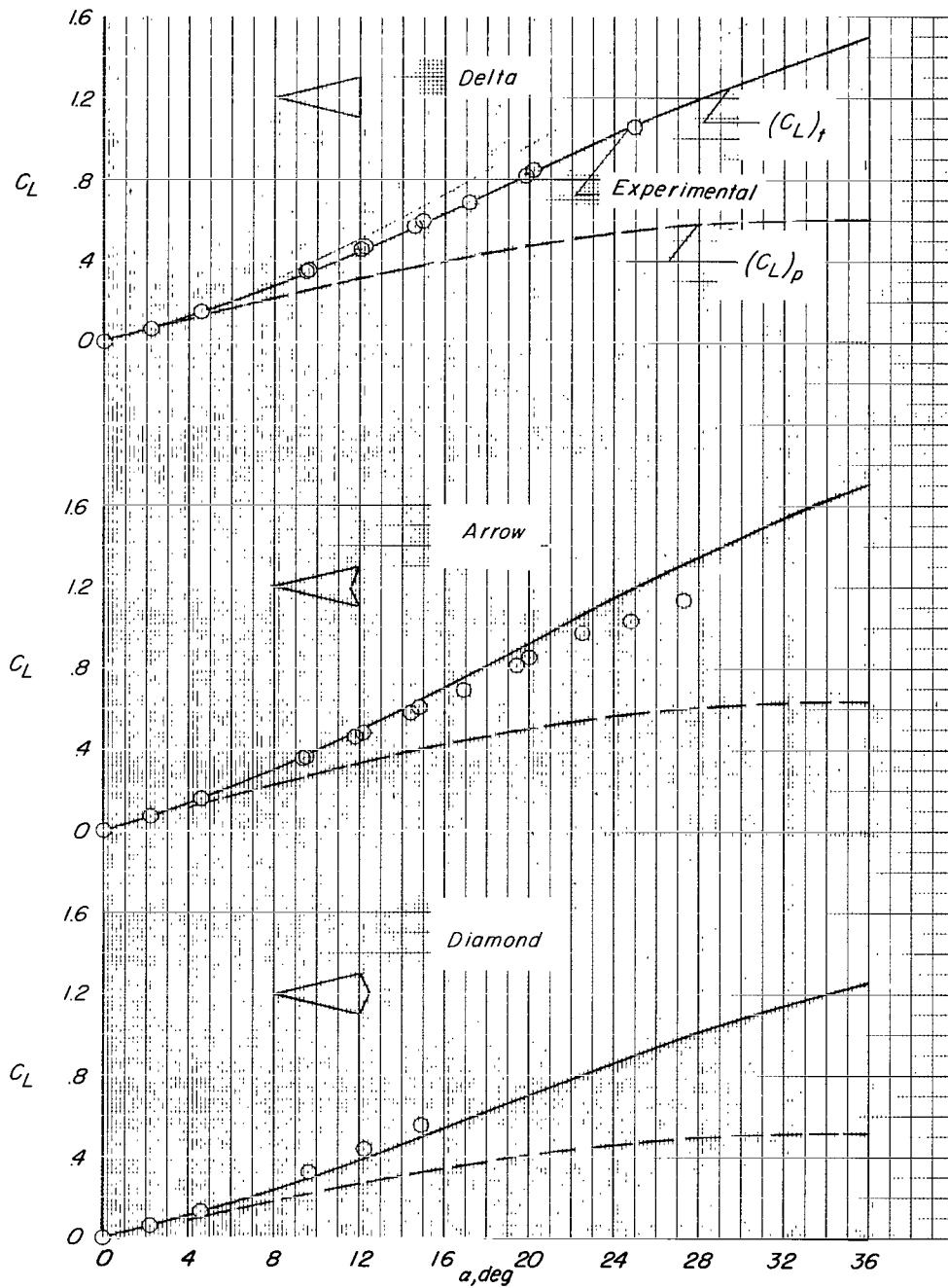
(d)   M = 0.8.
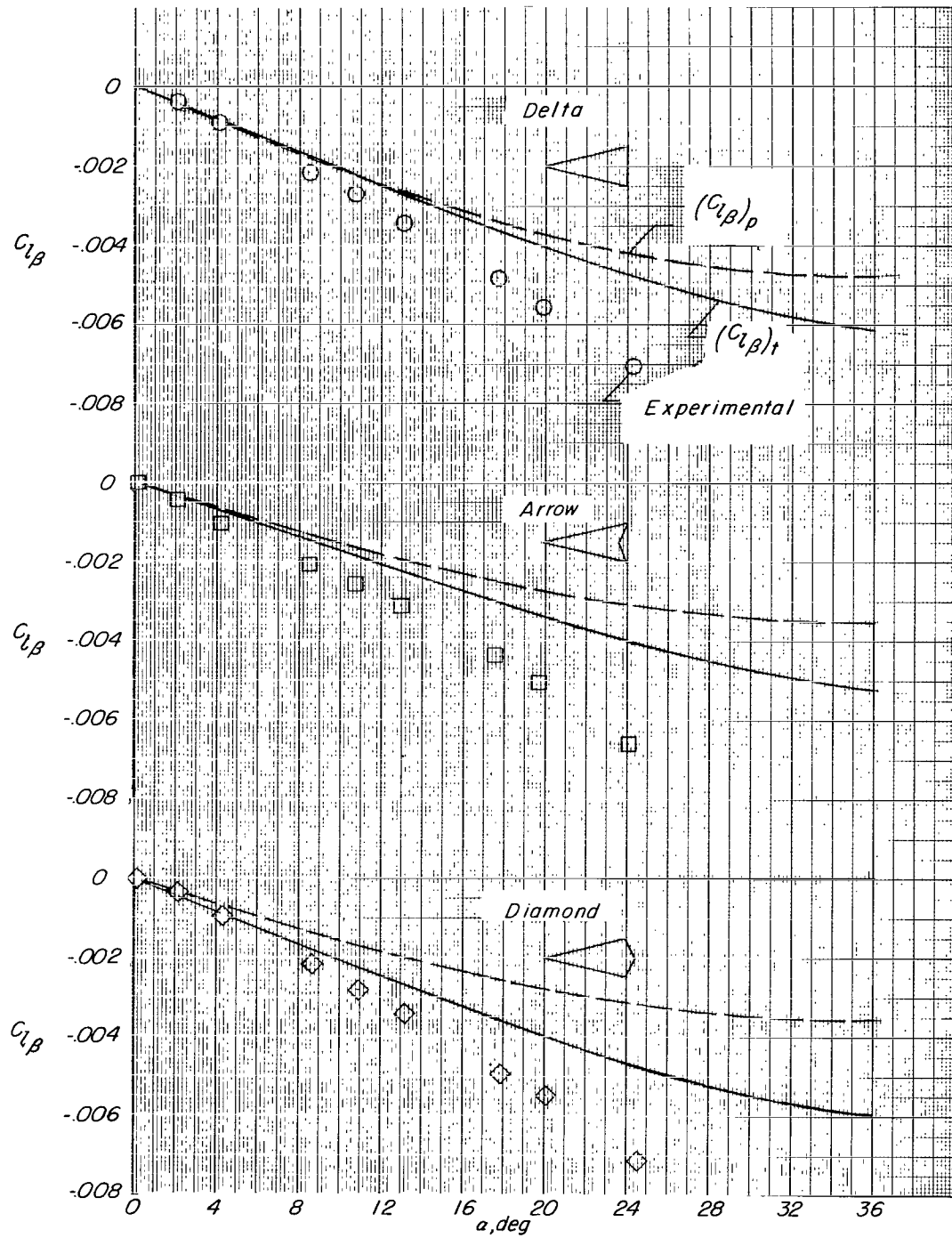
Figure 9.- Concluded.
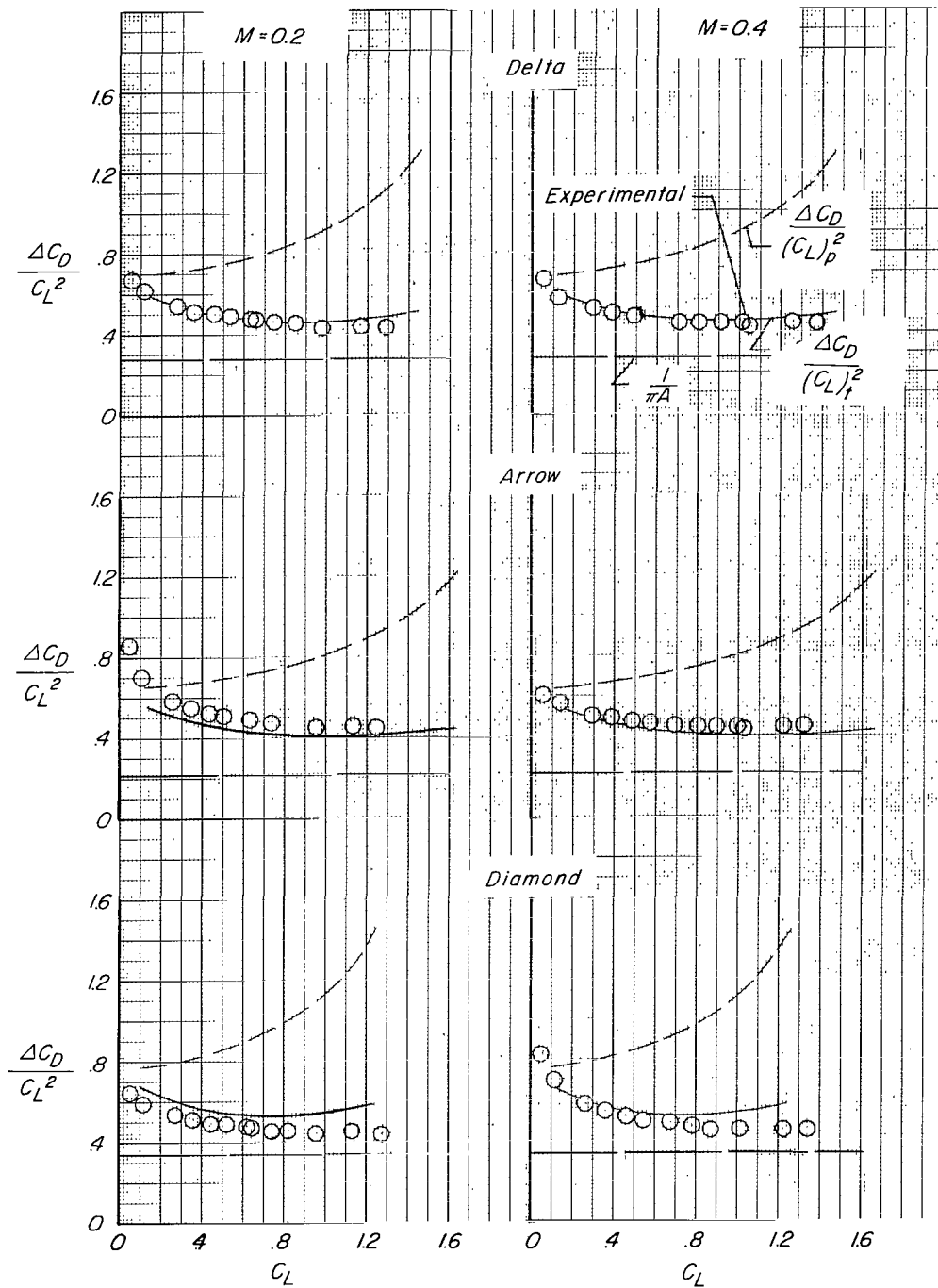
(a) M = 0.2 and 0.4.

Figure 10.- Theoretical and experimental drag-due-to-lift characteristics.
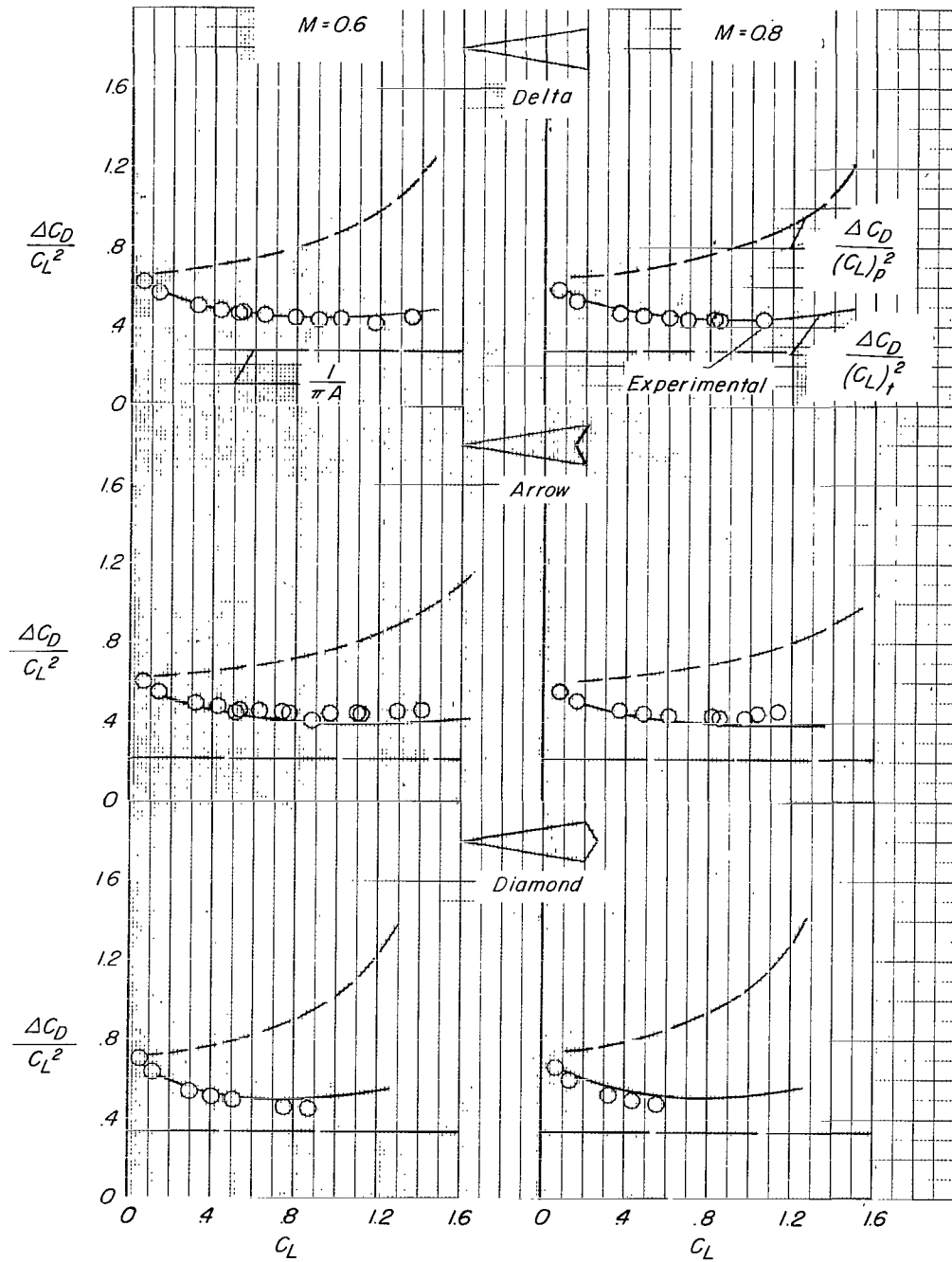
(b)   M = 0.6 and 0.8.

Figure 10.- Concluded.

Delta

Arrow

Diamond
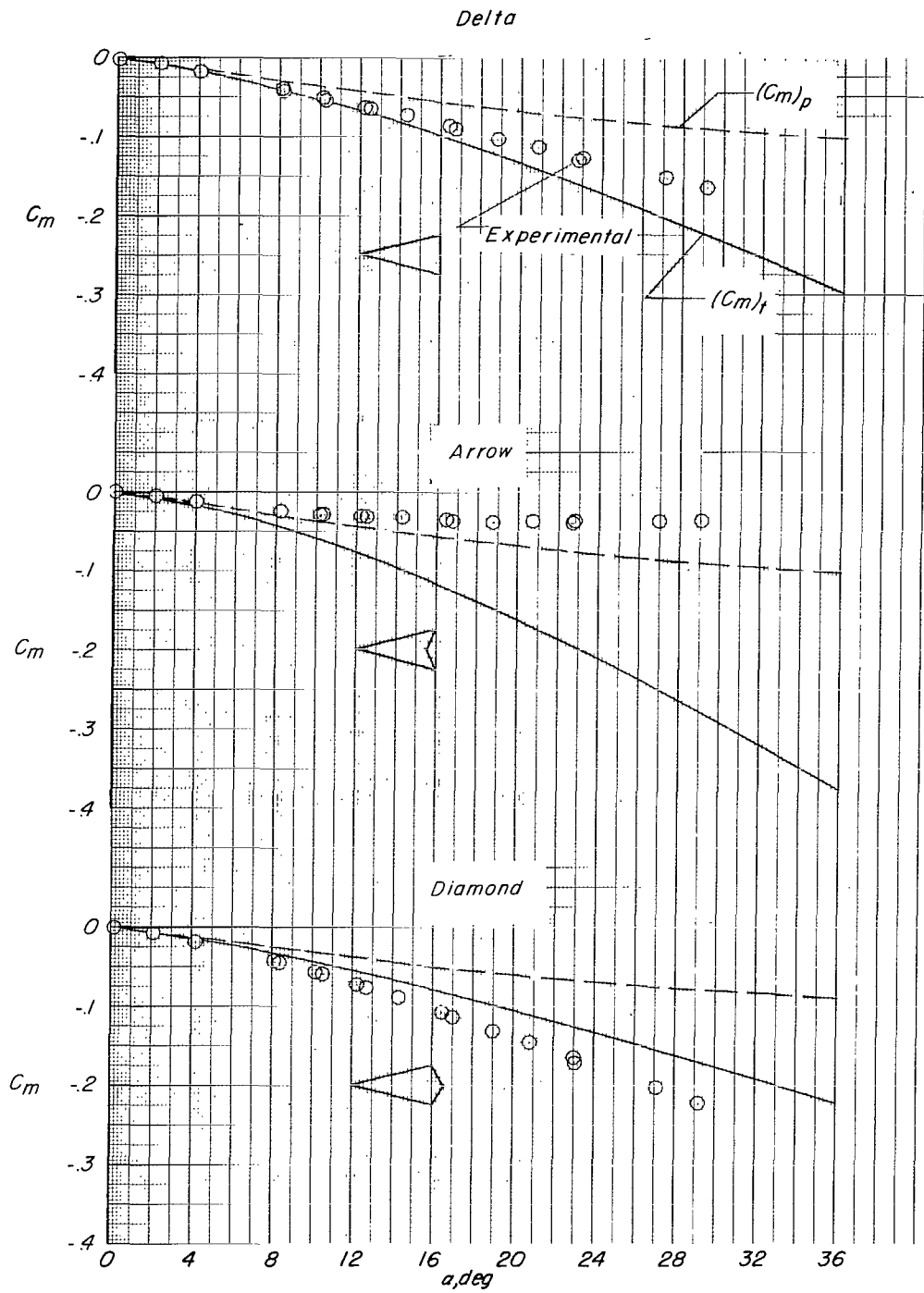
(a)   M = 0.2.

Figure 11.- Theoretical and experimental pitching-moment characteristics.

40

Delta

Arrow

Diamond
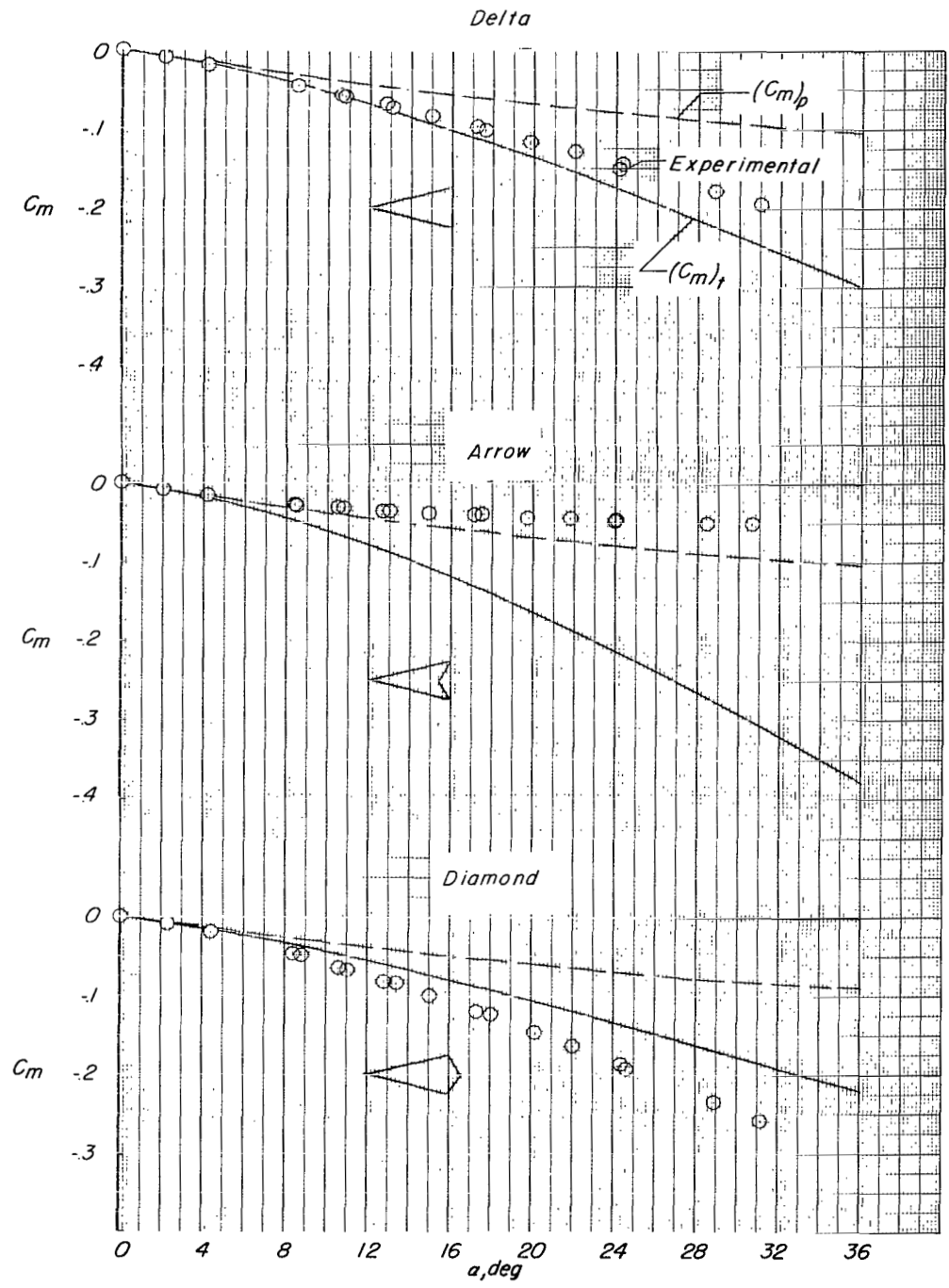
(b) M = 0.4.

Figure 11.- Continued.

(c)   M = 0.6.

Figure 11.- Continued.

(d) M = 0.8.

Figure 11.- Concluded.

Delta

$(C_{l_\beta})_p$

C_{l_β}

0

-.002

-.004

-.006

-.008

Experimental

$(C_{l_\beta})_t$

Arrow

C_{l_β}

0

-.002

-.004

-.006

-.008

Diamond

C_{l_β}

0

-.002

-.004

-.006

-.008

0   4   8   12   16   20   24   28   32   36

a,deg

(a) M = 0.2.

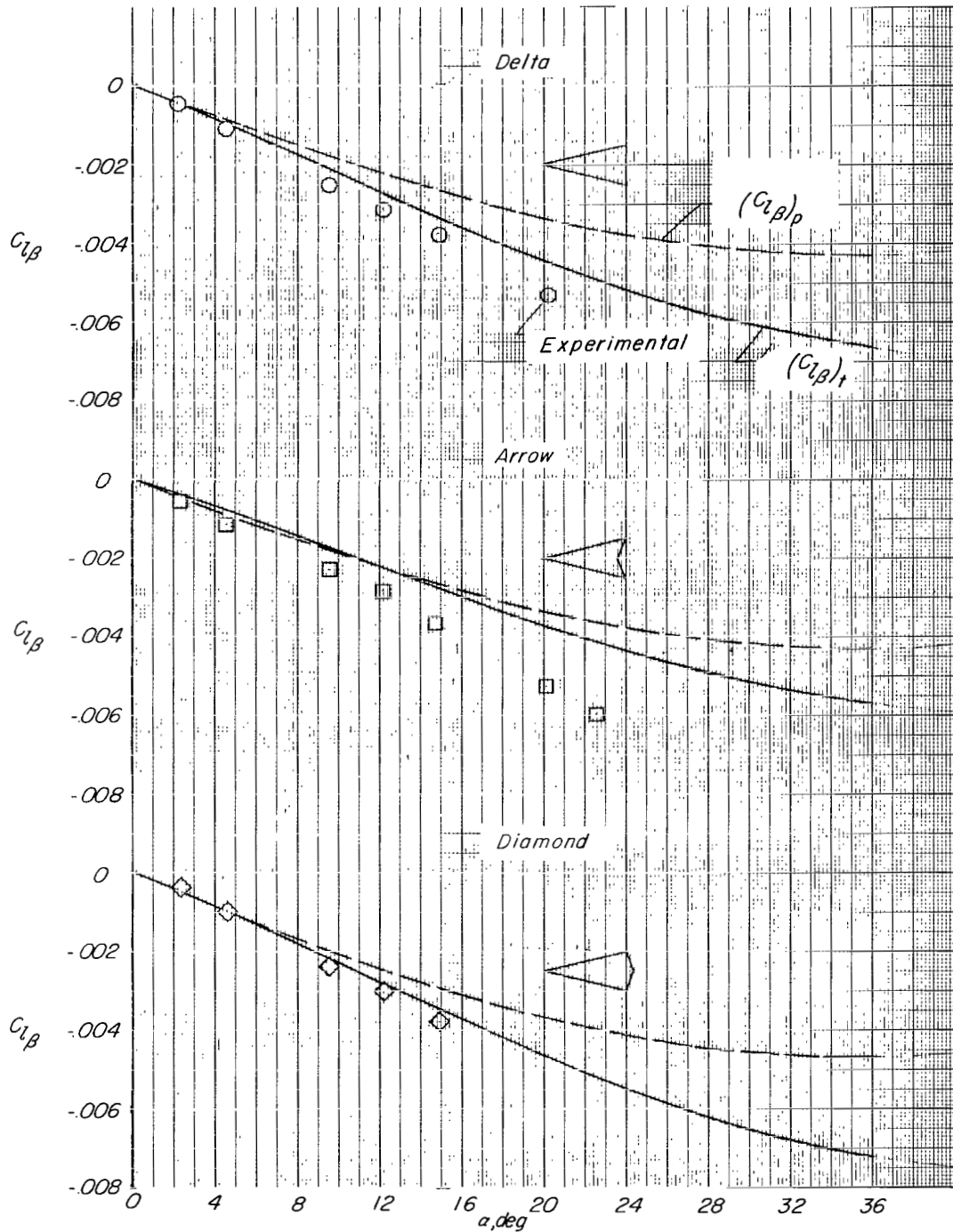Figure 12.- Predicted and experimental effective-dihedral parameters.

(b) M = 0.4.

Figure 12.- Continued.
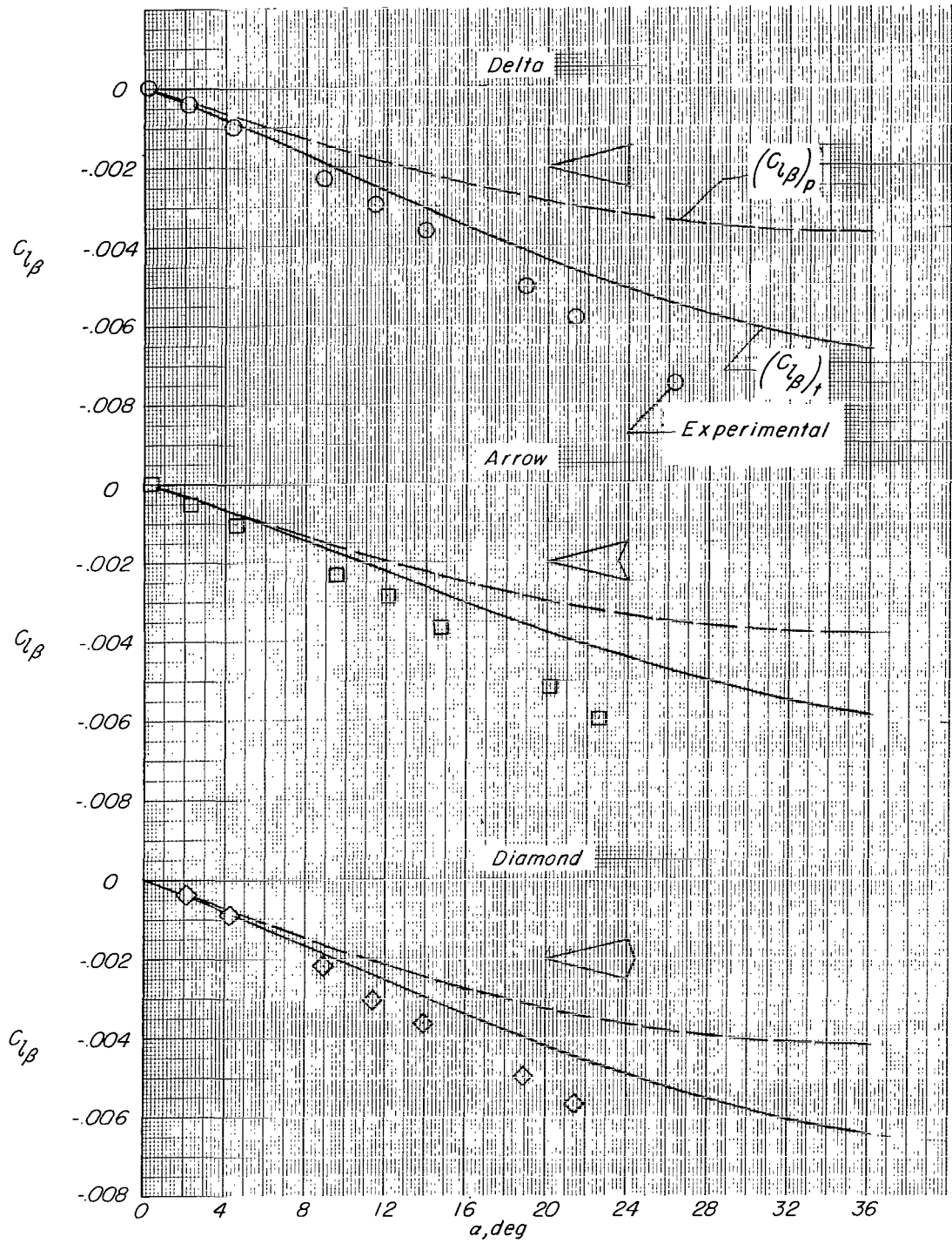
(c)   M = 0.6.

Figure 12.- Continued.

(d) M = 0.8.

Figure 12.- Concluded.
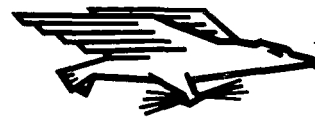
"The aeronautical and space activities of the United States shall be conducted so as to contribute . . . to the expansion of human knowledge of phenomena in the atmosphere and space. The Administration shall provide for the widest practicable and appropriate dissemination of information concerning its activities and the results thereof."

— NATIONAL AERONAUTICS AND SPACE ACT OF 1958

NASA SCIENTIFIC AND TECHNICAL PUBLICATIONS

TECHNICAL REPORTS: Scientific and technical information considered important, complete, and a lasting contribution to existing knowledge.

TECHNICAL NOTES: Information less broad in scope but nevertheless of importance as a contribution to existing knowledge.

TECHNICAL MEMORANDUMS: Information receiving limited distribution because of preliminary data, security classification, or other reasons.

CONTRACTOR REPORTS: Scientific and technical information generated under a NASA contract or grant and considered an important contribution to existing knowledge.

TECHNICAL TRANSLATIONS: Information published in a foreign language considered to merit NASA distribution in English.

SPECIAL PUBLICATIONS: Information derived from or of value to NASA activities. Publications include conference proceedings, monographs, data compilations, handbooks, sourcebooks, and special bibliographies.

TECHNOLOGY UTILIZATION PUBLICATIONS: Information on technology used by NASA that may be of particular interest in commercial and other non-aerospace applications. Publications include Tech Briefs, Technology Utilization Reports and Technology Surveys.

Details on the availability of these publications may be obtained from:

SCIENTIFIC AND TECHNICAL INFORMATION OFFICE

NATIONAL AERONAUTICS AND SPACE ADMINISTRATION
Washington, D.C. 20546